Drug Delivery

ISSN: 1071-7544 (Print) 1521-0464 (Online) Journal homepage: www.tandfonline.com/journals/idrd20

Ketorolac, melatonin and latanoprost tri-loaded PLGA microspheres for neuroprotection in glaucoma

Miriam Ana González-Cela-Casamayor, María J. Rodrigo, Marco Brugnera, Inés Munuera, Teresa Martínez-Rincón, Catalina Prats-Lluís , Pilar Villacampa, Julián García-Feijoo, Luis E. Pablo, Irene Bravo-Osuna, Elena Garcia-Martin & Rocío Herrero-Vanrell

To cite this article: Miriam Ana González-Cela-Casamayor, María J. Rodrigo, Marco Brugnera, Inés Munuera, Teresa Martínez-Rincón, Catalina Prats-Lluís , Pilar Villacampa, Julián García-Feijoo, Luis E. Pablo, Irene Bravo-Osuna, Elena Garcia-Martin & Rocío Herrero-Vanrell (2025) Ketorolac, melatonin and latanoprost tri-loaded PLGA microspheres for neuroprotection in glaucoma, Drug Delivery, 32:1, 2484277, DOI: 10.1080/10717544.2025.2484277

To link to this article: https://doi.org/10.1080/10717544.2025.2484277

Published online: 11 Apr 2025.

DRUG DELIVERY
2025, VOL. 32, NO. 1, 2484277
https://doi.org/10.1080/10717544.2025.2484277

Taylor & Francis
Taylor & Francis Group

RESEARCH ARTICLE

OPEN ACCESS Check for updates

Ketorolac, melatonin and latanoprost tri-loaded PLGA microspheres for neuroprotection in glaucoma

Miriam Ana González-Cela-Casamayor[a,b*], María J. Rodrigo[c,d*], Marco Brugnera[a,b,e], Inés Munuera[c,d], Teresa Martínez-Rincón[d], Catalina Prats-Lluís[f], Pilar Villacampa[f], Julián García-Feijoo[g], Luis E. Pablo[c,d], Irene Bravo-Osuna[a,b,e], Elena Garcia-Martin[c,d] and Rocío Herrero-Vanrell[a,b,e]

[a]Innovation, Therapy and Pharmaceutical Development in Ophthalmology (InnOftal) Research Group, UCM 920415, Department of Pharmaceutics and Food Technology, Faculty of Pharmacy, Complutense University of Madrid, Madrid, Spain; [b]Health Research Institute, San Carlos Clinical Hospital (IdISSC), Madrid, Spain; [c]Department of Ophthalmology, Miguel Servet University Hospital, Zaragoza, Spain; [d]Miguel Servet Ophthalmology Research Group (GIMSO), Aragon Health Research Institute (IIS Aragon), University of Zaragoza, Zaragoza, Spain; [e]School of Pharmacy, University Institute for Industrial Pharmacy (IUFI), Complutense University of Madrid, Madrid, Spain; [f]Department of Physiological Sciences, Faculty of Medicine and Health Sciences, University of Barcelona and Bellvitge Biomedical Research Institute (IDIBELL), l'Hospitalet de Llobregat, Spain; [g]Department of Ophthalmology, San Carlos Clinical Hospital, Health Research Institute of the San Carlos Clinical Hospital (IdISSC), Madrid, Spain

ABSTRACT

Glaucoma is a multifactorial neurodegenerative disease that affects the retina and optic nerve. The aim of this work was to reach different therapeutics targets by co-encapsulating three neuroprotective substances with hypotensive (latanoprost), antioxidant (melatonin) and anti-inflammatory (ketorolac) activity in biodegradable poly (lactic-co-glycolic acid) (PLGA) microspheres (MSs) capable of releasing the drugs for months after intravitreal injection, avoiding the need for repeated administrations. Multi-loaded PLGA MSs were prepared using the oil-in-water emulsion solvent extraction-evaporation technique and physicochemically characterized. PLGA 85:15 was the polymer ratio selected for the selected formulation. Tri-loaded MSs including vitamin E as additive showed good tolerance in retinal pigment epithelium cells after 24 h exposure (>90% cell viability). The final formulation (KMLVE) resulted in 33.58 ± 5.44 µm particle size and drug content (µg/mg MSs) of 39.70 ± 5.89, 67.28 ± 4.17 and 7.51 ± 0.58 for melatonin, ketorolac and latanoprost respectively. KMLVE were able to release in a sustained manner the three drugs over 70 days. KMLVE were injected at 2 and 12 weeks in Long-Evans rats (n = 20) after the induction of chronic glaucoma. Ophthalmological tests were performed and compared to not treated glaucomatous (n = 45) and healthy (n = 17) animals. Treated glaucomatous rats reached the lowest intraocular pressure, enhanced functionality of bipolar and retinal ganglion cells and showed greater neuroretinal thickness by optical coherence tomography ($p < 0.05$) compared to not treated glaucomatous rats at 24 weeks follow-up. According to the results, the tri-loaded microspheres can be considered as promising controlled-release system for the treatment of glaucoma.

ARTICLE HISTORY
Received 3 December 2024
Revised 17 March 2025
Accepted 20 March 2025

KEYWORDS
Ketorolac; melatonin; latanoprost; microspheres; neuroprotection; glaucoma

1. Introduction

Glaucoma, one of the main causes of irreversible blindness, is a multifactorial neurodegenerative disorder which courses with a gradual degeneration of retinal ganglion cells (RGCs) and their axons in the optic nerve (Meier-gibbons and Marc 2020). There are several types of glaucoma, being open-angle glaucoma (OAG) the most frequent one (Tanito *et al.* 2018). Currently, the most important modifiable risk factor for the development of OAG is the increased intraocular pressure (IOP). For this reason, the treatment of the disease is mainly focused on the topical administration of hypotensive drugs, which act by increasing the drainage of aqueous humor or decreasing its production. Currently, there are numerous hypotensive eye drops on the market for the treatment of glaucoma, aimed at reducing intraocular pressure (Alm 2014).

However, one of the major problems with the ocular topical route is the low local bioavailability, which results in increased frequency of instillation, and therefore poor patient compliance and important adverse effects such as the development of dry eye disease (DED) (Davies 2000, Actis and Rolle 2014, del Amo 2022, Ghosh *et al.* 2024). In addition, control of intraocular pressure does not always avoid retinal degeneration, in fact it is worth mentioning that glaucomatous processes also occur in normotensive patients (normotensive glaucoma). In this context, neuroprotective therapies emerge to prevent or delay glaucomatous neurodegeneration, thus preventing the progression of blindness whatever

CONTACT Rocío Herrero-Vanrell rociohv@ucm.es Department of Pharmaceutics and Food Technology, Faculty of Pharmacy, Complutense University of Madrid, 28040 Madrid, Spain.
*These authors contributed equally to this work.

the origin of the disease (Chidlow *et al.* 2007, Review 2014). Numerous strategies have been pursued for neuroprotection. The most frequent therapeutic targets are glutamate receptors, potentiation of protective autoimmunity, neurotrophin deprivation, nitric oxide synthesis, voltage-gated sodium and calcium channels, oxidative stress, heat shock proteins, inflammation and retinal ganglion cell death and apoptosis (Chidlow *et al.* 2007).

Due to the presence of ocular barriers, intravitreal injections are needed to reach the posterior segment of the eye and provide neuroprotection. However, they have important disadvantages associated with the intravitreal route itself such as high cost, invasiveness or potential local adverse effects, which are further increased by the fact that multiple injections are required to maintain therapeutic drug levels in the retina and surrounded tissues (Bhanu *et al.* 2017).

Intraocular drug delivery systems (IODDS) have been raised as therapeutic platforms to overcome this limitation. IODDS are capable of releasing active ingredients over long periods, thus avoiding the need for frequent repeated injections (Alhalafi 2017). The use of IODDS is a solution to reduce the cost and adverse effects of repeated interventions while maximizing therapeutic efficacy. Biodegradable IODDS are preferred, since, upon injection, they can release the active ingredient while degrading, without the need to be removed. Of particular interest in IODDS is the use of poly (lactic) acid (PLA) and poly (lactic-co-glycolic) acid (PLGA), approved by the FDA and the EMA for intraocular systems (Nguyen *et al.* 2020, Wang *et al.* 2021). Nowadays the use of PLGA for the development of biodegradable microspheres which enable to encapsulate low and high molecular weight substances is increasing (Alhalafi 2017, Bravo-osuna *et al.* 2018).

Among the different active ingredients used to reduce IOP, the most common are prostaglandin 2 analogues (PGE2) such as latanoprost (Lat), bimatoprost or travoprost, which decrease the IOP by increasing the aqueous humor outflow (Doucette and Walter 2017). Prostaglandin analogues have not only hypotensive effect but neuroprotective one. The retinal neuroprotective effect of prostaglandin analogues such as latanoprost has been revealed in different studies. In fact, it has been described that prostaglandins may influence cyclo-oxygenase (COX-2) and nitric oxide (NO) synthase activity, thus interfering with the ischemia-induced neurotoxic processes that appear in glaucoma (Drago *et al.* 2001). Also, Kudo *et al.* (2006) not only showed the neuroprotective effect of intravitreal administered latanoprost in NMDA-induced RGC damage animal model, but also in optic nerve axotomy animal models (Kudo *et al.* 2006). Kanamori *et al.* (2009) demonstrated an anti-apoptotic effect of latanoprost acid on RGCs in an animal model of optic nerve crush. According to these authors, it seems evident that the drug can reduce intracellular calcium concentrations and therefore the activation of caspase 3 (Kanamori *et al.* 2009). Furthermore, recent studies have shown that latanoprost is also capable of inducing the expression and shedding of klotho proteins in RGC, which in turns may contribute not only to the attenuation of axonal injury-induced calpain activation but also to the reduction of oxidative stress, thereby protecting the RGCs against posttraumatic neuronal degeneration (Yamamoto *et al.* 2017). It seems very probably that the neuroprotective activity of latanoprost in vivo may be the result of multiple action on different biological targets (Drago *et al.* 2001), however the complex neuroprotective mechanisms of latanoprost remain still unknown.

Melatonin (N-acetyl-5-methoxytryptamine) (Mel) is a neuroprotectant proved in retinal degenerative diseases (Ye *et al.* 2022). It is an active ingredient with antioxidant properties that has been shown in numerous studies to have neuroprotective activity in retinal degeneration produced in glaucoma disease (Belforte *et al.* 2010, Reiter *et al.* 2016). In fact, melatonin has been shown to have a neuroprotective and antiapoptotic effect thanks to the reduction of damage from oxidative stress (Bessone *et al.* 2019, 2020). In addition, melatonin has been proposed to help regulate the circadian rhythms and reduce the IOP (Saniples *et al.* 2000).

Furthermore, although the mechanisms involving inflammation in glaucoma are not yet fully understood, it is known that it plays an important role in neurodegeneration RGCs (Maranha 2020). The non-steroidal anti-inflammatory drugs (NSAIDs) such as Ketorolac (Ket) (that inhibit the enzyme cyclooxygenase) is a safe and effective agent already tested to treat the ocular inflammation. Previously, it has been shown that ketorolac was able to protect RGCs in vivo after axonal damage (Nadal-Nicolás *et al.* 2016). In addition, other authors have found that the use of the anti-inflammatory drug ketorolac may improve the IOP-lowering effect in patients treated with latanoprost (Costagliola *et al.* 2008, Turan-Vural *et al.* 2012).

The aim of this work was to combine different neuroprotective compounds (ketorolac, melatonin and latanoprost) in a single microparticulate multi-functional controlled release system for the treatment of glaucoma, with the objective to obtain a long-term (6 months) protection of the neuroretina in glaucomatous rats. The animal model of chronic glaucoma used in this study was previously developed by some of the authors (Aragón-Navas *et al.* 2022).

2. Material and methods

2.1. Materials

The active substances ketorolac and melatonin with high purity were supplied by Merck (Darmstadt, Germany), as well as vitamin E 96% and Polyvinyl alcohol 67,000 g/mol (PVA). Latanoprost was from Quimigen (Madrid, Spain). Different types of poly(d,l-lactide-co-glycolide) (PLGA) were purchased from Evonik (Darmstadt, Germany): PLGA 503, 503H 735 S, 735H, 85:15. The mobile phases were prepared with methanol and acetonitrile HPLC grade provided by PanReac (AppliChem, Barcelona, Spain).

2.2. PLGA microspheres preparation

The microencapsulation of the different compounds was performed by the oil/water emulsion solvent extraction-evaporation technique (Brugnera *et al.* 2022). For the manufacture of the formulations, 400 mg of PLGA were dissolved in

0.7 mL of dichloromethane (DCM). After that, the active ingredients were added together with 25% v/v (232 µL) ethanol for dissolution (total organic solvents volume 932 µL). Subsequently, the mixture was subjected to cold ultrasonication for 5 minutes and stirred with a sonication probe for 1 minute at 4 °C, forming the final O-phase. To create the emulsion, the external aqueous phase, composed of 2% polyvinyl alcohol (PVA) in MilliQ® water, was added (5 mL) and the emulsion was formed at 10,000 rpm during 2 minutes in a homogenizer (Polytron®RECO, Kinematica, GmbHT PT3000, Lucerna, Switzerland). The subsequent maturation took place for 3 hours in an agitation bath at room temperature, using 0.1% PVA in water as maturation phase, until complete evaporation of the organic solvents. Finally, the desired microspheres fraction size (38-20 µm) was washed and collected using two sieves (38 and 20 µm size). The particles were freeze-dried (Freezing at −80 °C for 15 min and drying at −80 °C and 0.1 mBar for 12 hours. MSs were stored under dry conditions at −30°C.

The PLGA polymers used were of different lactic-glycolic ratios and molecular weights: PLGA 503, 503H, 735S, 735H and PLGA 85:15. The first step of the optimization process consisted in the selection of the polymer more suitable for the microencapsulation of fixed amounts of ketorolac and melatonin (60 mg and 80 mg respectively). After that, the addition of vitamin E (40 µL) and the antihypertensive agent latanoprost (4 mg) was performed.

2.3. Latanoprost, ketorolac and melatonin quantification by HPLC

The quantification of the different drugs was carried out using two different methods. For simultaneous melatonin and ketorolac quantification, a method previously validated by our group was used (Brugnera *et al.* 2022). Briefly, the mobile phase was composed of methanol and 50 mM ammonium formate solution (adjusted with formic acid to pH 4) in a 60:40 ratio. The quantification was performed with an Ascentis® C18 25 cm × 4.6 mm × 5 µm column. The flow was 1 mL/min and the analysis time was 8 minutes. The column temperature was maintained at 45 °C. The wavelengths of maximum absorption were 313.5 nm for ketorolac and 222.5 for melatonin.

For the quantification of latanoprost, a method previously described by other authors with some modifications was used (Mansoor and Tas 2014). The mobile phase was composed of acetonitrile and 0.1% v/v trifluoroacetic acid (TFA) adjusted at pH 3 in water in a 70:30 ratio. The flow was 1 mL/min and the analysis time was 3 minutes. The column used for this analysis was a Ascentis® C18 10 cm x 4.6 mm x 3 µm. The wavelength of maximum absorption was 205.0 nm.

2.4. Microspheres characterization

2.4.1. Mean particle size and particle distribution

Dual light scattering technique (Microtrac® S3500 Series Particle Size Analyzer, Montgomeryville, PA, USA) was used to obtain the mean particle size and size distribution of the MSs. The measurements were performed in triplicate and expressed in volume mean diameters ± standard deviation.

2.4.2. Morphology evaluation of MSs

For morphology evaluation scanning electron microscopy (SEM, Jeol, JSM-6335F, Tokyo, Japan) was used. MSs were coated with a gold sputter-coating for 60 seconds for external surface observation.

2.4.3. Encapsulation efficiency

The encapsulation efficiency of the formulations (EE%), understood as the drug successfully entrapped into the MSs, was performed by adding 1 mL dichloromethane (DCM) to 1 mg of MSs and stirred with vortex for 30 seconds to dissolve the PLGA. Subsequently 2.5 mL MeOH were added, and the mixture was stirred for 1 minute to precipitate the PLGA. The resulting solution of the active compounds in the DCM:MeOH mixture was centrifuged at 5000 rpm for 10 minutes and filtered through a 0.22 µm pore size nylon filter (JNY022013N, Filter-Lab®, Barcelona, Spain). Finally, the samples were quantified by HPLC. The EE of the drugs were calculated individually as the ratio of the actual amount of drug per weight of MSs to the total weight of drug added during the processing of the microspheres.

$$EE\left(\frac{\mu g}{\text{mg MSs}}\right)=\frac{\mu g\,\text{Drug}}{mg\,MSs\,weighted}$$

$$EE(\%)=\frac{\dfrac{\text{mg Drug}}{\text{mg MSs } weighted}}{\dfrac{mg\ Drug\ added}{mg\ Drugs\ added+mg\ PLGA\ added}}\times 100\%$$

2.5. In vitro release studies

For in vitro release studies, 5 mg of MSs loaded with active ingredients were weighed into Eppendorf tubes. Then, 2 mL of Phosphate-buffered saline (PBS), a buffer solution with 7.4 pH, was added. In all cases, the volume was sufficient to maintain sink conditions for the active ingredients. As an exception, for the study of the in vitro release of latanoprost 10 mg MSs were added due to the low amounts of latanoprost present in the MSs, which makes subsequent quantification difficult.

To quantify the released drugs, the PBS solution was removed after 24 h (burst), and every 7 days after centrifugation for 5 min at 5000 rpm. The supernatants were filtered with a 0.22 µm nylon filter. Fresh 2 mL of PBS was added to the tubes and the remaining microspheres were gently resuspended to continue the assay. For the quantification of melatonin and ketorolac, the solutions in PBS were directly quantified by HPLC with the appropriate dilution. On the other hand, for the quantification of latanoprost, the 2 mL of solution was lyophilized until the complete elimination of water, and subsequently dissolved in 0.5 mL of acetonitrile.

To compare the release profiles, we use the similarity factor (f2). Using f2, it can be established that the difference between the two release profiles is lower than 10% when values are between 50 and 100.

$$f2 = 50.\log\left[\frac{100}{\sqrt{1+\frac{\sum_{t=t}^{t=n}\left[\bar{R}(t)-\bar{T}(t)\right]^2}{n}}}\right]$$

2.6. In vitro cytotoxicity studies

2.6.1. Cell cultures

Human retinal pigment epithelium cells (RPE-1) donated by the UCD (University College of Dublin) were used for in vitro studies. Cells were cultured using a culture medium of Dulbecco's Modified Eagle Medium/Nutrient Mixture F-12 (DMEM F-12) supplemented with 1% penicillin-streptomycin, 1% L-glutamine, 3,5% sodium bicarbonate 7,5% solution and 10% fetal bovine serum (FBS). Cells were incubated at 37 °C and 5% CO2. Cells were cultured to approximately 80% confluence, at which point cells were transferred into new T-75 flasks. Cells were detached from the T-75 flask using trypsin in EDTA (1 mL for 5 minutes). The detached cells were then resuspended and centrifuged at 850× g for 10 minutes in a 15 mL falcon to obtain a pellet. Finally, the pellet was resuspended, and the desired number of cells was added to a new T-75 flask. The passages used for the assays were 10–25.

2.6.2. Cytotoxicity assay

The cytotoxicity study was carried out by seeding the cells in a 96-well plate at a density of 7,000 cells per well. Culture medium was used as a negative control (established as 100% cell viability) and dimethyl sulfoxide (DMSO) 10% was used as positive control (Javier *et al.* 2021). The method for assessing the cytotoxicity of the formulations was the MTT method, studying the mitochondrial-dependent reduction of the tetrazolium salt 3-(4-5-dimethylthiazol-2-yl)-2,5-diphenyltetrazolium bromide) (MTT) to formazan crystals. For the toxicity of the microspheres and their components, studies were conducted using the blank microspheres (MSs B) and including vitamin E (MSs B VE), ketorolac (MSs-Ketorolac), melatonin (MSs-Melatonin) and latanoprost (MSs-Latanoprost) alone, co-loaded with ketorolac and melatonin without (KM) and with vitamin E (KMVE) and tri-loaded with ketorolac, melatonin and latanoprost with with vitamin E (KMLVE).

For the assay the plates were seeded, and the cells were allowed to grow overnight. Subsequently, the culture medium was removed and 100 µL of new culture medium was added to each well. Then, 100 µL of MSs suspension in culture medium was added at a concentration of 1 mg/mL to give a final concentration of 0.5 mg/mL (negative control columns were supplemented with 100 µl of culture medium, and the positive control columns with 100 µl of 10% DMSO). The exposure to microspheres lasted 24 hours. After that, the culture medium and compounds were removed and 100 µL/well of 0.83% MTT solution was added to the 96-well plate. After 2 hours of exposure, MTT was removed and the formazan salt crystals formed were dissolved using 100 µL/well of DSMO. The plate was read in a spectrophotometer at 550 nm wavelength.

2.7. In vivo studies

This is a longitudinal and interventionist study for evaluating the effectiveness of KMLVE in a steroid induced glaucoma model. Long-Evans rats were supplied from Javier Labs (Le Genest-Saint-Isle, France). Three different cohorts were assayed: healthy rats ($n=17$), rats with chronic glaucoma ($n=45$) and glaucomatous rats ($n=20$) treated with intravitreal injections (IV) of tri-loaded PLGA-MSs (latanoprost-melatonin-ketorolac) selected from *in vitro* studies (KMLVE). The chronic glaucoma in rats was induced by a single intracameral injection of biodegradable PLGA-MSs loaded with dexamethasone (Dexa) and fibronectin (Fibro) being previously reported (Aragón-Navas *et al.* 2022).

All work with animals was performed in accordance with the Association for the Research in Vision and Ophthalmology (ARVO) statement on the Use of Animals and the ARRIVE (Animal Research: Reporting of *In Vivo* Experiments) guidelines. Moreover, *in vivo* studies were approved by the Ethics Committee for Animal Research (P179/20) and are part of a broader research project approved under a unified Ethics Approval code, which may result (or has resulted) in multiple related publications. The study was carried out in the experimental surgery department of the Biomedical Research Center of Aragon (CIBA), located in Zaragoza, Spain. A total of 82 Long-Evans rats (50% males/50% female) aged 4 weeks-old and weighted ranged from 50-100 g at the beginning of the study were used. The environmental conditions were controlled: 12-hour light/dark cycles, temperature of 22 °C, relative humidity of 55% and housed in standard cages with environment enrichment, water and food *ad libitum*.

2.7.1. Injection procedures

Chronic glaucoma was induced by a single injection of 2 µL PLGA Ms-Dexa-Fibro suspension (10% w/v) administered through the cornea into the anterior chamber of the right eye, using a micrometer Hamilton® syringe with a glass micropipette at baseline. Treated animals received two injections (2 µL) of KMLVE- suspension (5%w/v) into vitreous chamber at 2 and 12 weeks after glaucoma induction. All injections were performed by specialists in Ophthalmology, under aseptic conditions. During procedures temperature was controlled with warm pads, and after that animals were left to recover in an oxygen-enriched (2.5%) atmosphere. Evaluation of IOP and *in vivo* neuroretinal structure by optical coherence tomography (OCT) and functionality by electroretinography (ERG) was performed throughout 24 weeks.

2.7.2. Anesthesia

For corneal and intravitreal injections and IOP measurements rats were previously sedated with a mixture of 3% sevoflurane gas and 1.5% oxygen. For ERG and OCT acquisitions general anesthesia by intraperitoneal injections of ketamine

(60 mg/kg) and dexmedetomidine (0.25 mg/kg) was used, but also topical anesthesia with 1 mg/mL tetracaine + 4 mg/mL oxiburprocaine (Anestesico doble Colircusi®, Alcon Cusi® SA, Barcelona, Spain), and animal's pupils were fully dilatated with tropicamide (10 mg/ml) and phenylephrine (100 mg/ml) (Alcon Cusi® SA, Barcelona, Spain).

2.7.3. In vivo ophthalmological tests

IOP was assessed by a Tonolab® tonometer (Tonolab, Tiolat Oy Helsinki, Finland). Six measurements were taken and averaged in each eye. Examinations were always done in all rats in the afternoon to avoid circadian fluctuation pattern, in both right and left eyes (always measuring right eye first). Measurements from healthy animals were taken at 0, 4, 12 and 24 weeks. To deepen characterization of the formulation effectiveness in both cohorts with chronic glaucoma non-treated and treated were taken at baseline, 2, 4, 6, 12, 18 and 24 weeks of follow-up.

ERG (Roland consult RETIanimal® ERG, Germany) was used to study neuroretinal functionality, measuring signal latency (in ms) and amplitude (in µV). Flash scotopic ERG and photopic negative responses (PhNR) protocols were performed. For scotopic ERG the animals were dark-adapted for 12 hours. Electrodes were placed as described: active ones on both right and left corneas, references on both body sides under skin and the ground one near the tail. Acceptable impedance was considered if less than 2kΩ between electrodes. Both eyes were simultaneously tested using a Ganzfeld Q450 SC sphere stimulated by white LED flashes. There were performed 7 steps to analyze rod response (step 1: -40dB, 0.0003 cds/m^2, 0.2 Hz [20 recordings averaged], step 2: -30dB, 0.003 cds/m^2, 0.125 Hz [18 recordings averaged], step 3: -20dB, 0.03 cds/m^2, 8.929 Hz [14 recordings averaged], step 4: -20dB, 0.03 cds/m^2, 0.111 Hz [15 recordings averaged], step 5: -10dB, 0.3 cds/m^2, 0.077 Hz [15recordings averaged]), mixed rod-cone response (step 6: -40dB, 3.0 cds/m^2, 0.067 Hz [12 recordings averaged], and oscillatory potentials (step 7: 0dB, 3.0 cds/m^2, 29.412 Hz [10 recordings averaged]. PhNR test was performed after light adaptation to a blue background (470 nm, 25 cds/m^2) stimulated with a red LED flash (625 nm, -10dB, 0.30 cds/m^2, 1.199 Hz [20 recordings averaged]. Six animals (both sexes) were tested at baseline, 12 and 24 weeks of follow- up.

Neuroretinal structure was analyzed by OCT (Spectralis®, Heidelberg Engineering, Germany), quantifying retinal parameters thickness in micrometers (µm). Segmentation protocols were performed for the analysis of Retina Posterior Pole (RPP), Ganglion Cell Layer (GCL) and peripapillary Retinal Nerve Fiber Layer (pRNFL). These protocols use 61 scans to analyze an area centered on the optic disk, since these animals do not have macula. The RPP and GCL protocols analyze a 3 mm^2 area including 9 EDTRS (Early Disease Treatment Retinopathy Study) areas: a central ring (C) of 1 mm diameter, an inner ring of 2 mm diameter divided into inferior (II), superior (IS), nasal (IN) and temporal (IT) sectors and an outer ring of 3 mm diameter divided also into inferior (OI), superior (OS), nasal (ON) and temporal (OT) sectors. The pRNFL protocol analyzes 6 sectors: inferotemporal (IT), temporal (T), superotemporal (ST), superonasal (SN), nasal (N) and inferonasal (IN). A corneal-adapted contact lens power plane was used to acquire higher quality images. Measurements were taken in both eyes (always measuring right eye first). Six animals (both sexes) were tested at baseline, 6, 12, 18 and 24 weeks of follow-up. After each OCT examination at 12 and 24 weeks, the 6 animals were euthanized with an intracardiac injection of sodium thiopental (25 mg/mL) under general anesthesia, in accordance with humane conditions.

2.8. Histological studies

Their eyes were immediately enucleated and fixed with paraformaldehyde and stored at 4 °C in PBS. Then, eyes were dehydrated and paraffin-embedded for sectioning (5 µm) along the eye axis, deparaffinized and rehydrated. After several washes in phosphate buffered saline (PBS), permeabilization and blocking steps, sections were incubated overnight at 4 °C with the following primary antibodies: anti-Brn3a (14A6, Santa Cruz Biotechnology), 1:50; anti-GFAP (Z0334, Agilent, Dako), 1:500. Immunohistochemistry controls were performed by omission of the primary antibody in a sequential tissue section. After washes, slides were incubated with the required secondary antibodies followed by Hoescht (Thermo Fischer Scientific) for nuclei counterstaining. Slides were mounted in Shandon Immu-Mount (Thermo Fischer Scientific) medium for microscopic analysis. Microscopy was performed using an LSM 880 confocal microscope and Axio Imager M2 (Carl Zeiss). Confocal image stacks were processed and quantified with the ImageJ.

2.9. Statistical analysis

Data were recorded in an Excel database. Statistical analysis was performed using IBM SPSS version 20.0 (SPSS Inc, Chicago, IL). The Kolmogorov-Smirnov test was used to assess sample distribution. Since the non-nonparametric distribution, a Mann-Whitney U test was used to evaluate differences between groups. Values were expressed as mean standard deviation. Values of $p < 0.05$ (marked with an *) were considered statistically significant. The Bonferroni correction for multiple comparisons was applied to avoid a high false-positive rate.

3. Results

3.1. Polymer selection

3.1.1. Microspheres characterization

3.1.1.1. Size and morphology. The mean particle size observed in the selected size fraction of microspheres co-loaded with melatonin and ketorolac prepared with the different PLGA polymers resulted between 28 and 34 µm (Table 1). There were no significant differences in size between MSs prepared with different polymers ($p > 0.05$) with unimodal particle size distribution.

According to SEM pictures, all formulations resulted in spherical structure with smooth non-porous surfaces and free of crystals (Figure 1).

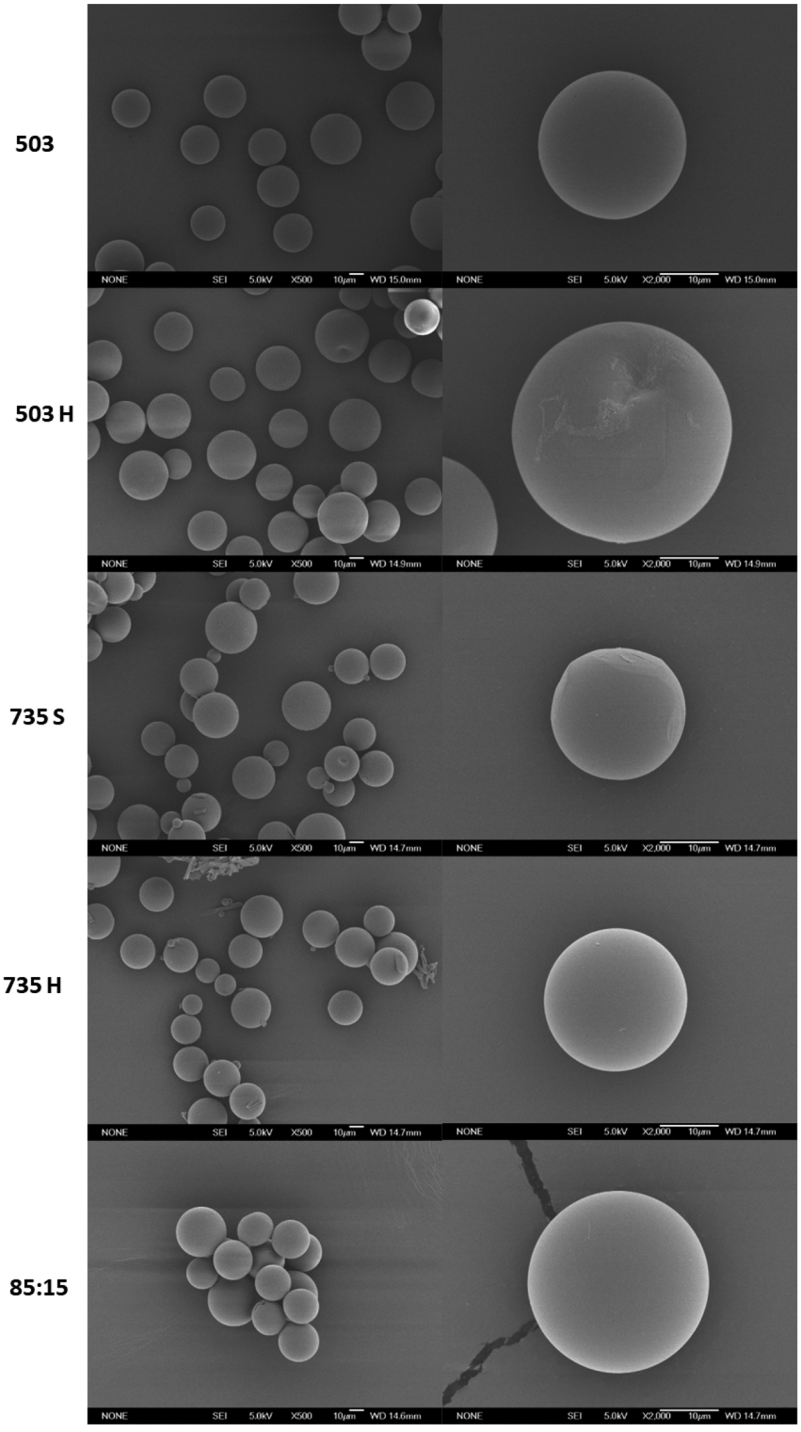

Figure 1. MSs elaborated with different types of PLGAs prepared from 60 mg ketorolac and 80 mg melatonin visualized by scanning electron microscopy.

Table 1. Mean size [µm ± SD] and encapsulation efficiency (EE) [µg/mg MSs and %] of melatonin and ketorolac in MSs developed with different polymers (mean ± SD).

Polymer	Particle size (µm ± SD)	EE [µg/mg ms]		EE [%]	
		Melatonin	Ketorolac	Melatonin	Ketorolac
503	31.07 ± 7.47	46.82 ± 3.88	65.48 ± 6.41	31.61 ± 2.63	58.69 ± 5.56
503 H	31.01 ± 6.84	58.48 ± 3.38	76.06 ± 0.49	39.38 ± 2.31	68.82 ± 1.09
735 S	29.73 ± 8.77	26.12 ± 1.63	52.83 ± 0.80	17.62 ± 1.08	47.48 ± 0.73
735 H	29.97 ± 6.97	49.59 ± 3.52	78.85 ± 1.87	33.45 ± 2.34	70.65 ± 1.62
85:15	30.04 ± 6.51	39.55 ± 3.15	67.24 ± 5.32	26.68 ± 2.11	60.46 ± 4.67

3.1.1.2. Encapsulation efficiency. Melatonin and ketorolac in the microspheres were quantified as described in the Materials and Method section (Table 1). Ketorolac encapsulation efficiency resulted significantly higher ($p < 0.05$) for the two polymers with carboxy-terminal groups in comparison to the other PLGAs employed while melatonin, presented the same behavior for MSs prepared with 503H, with significant higher EE values ($p < 0.05$) than MSs prepared with the other polymers (503: $p = 0.02$, 735S: $p = 0.0001$, 85:15: $p = 0.002$, 735H $p = 0.034$). However, for MSs prepared with

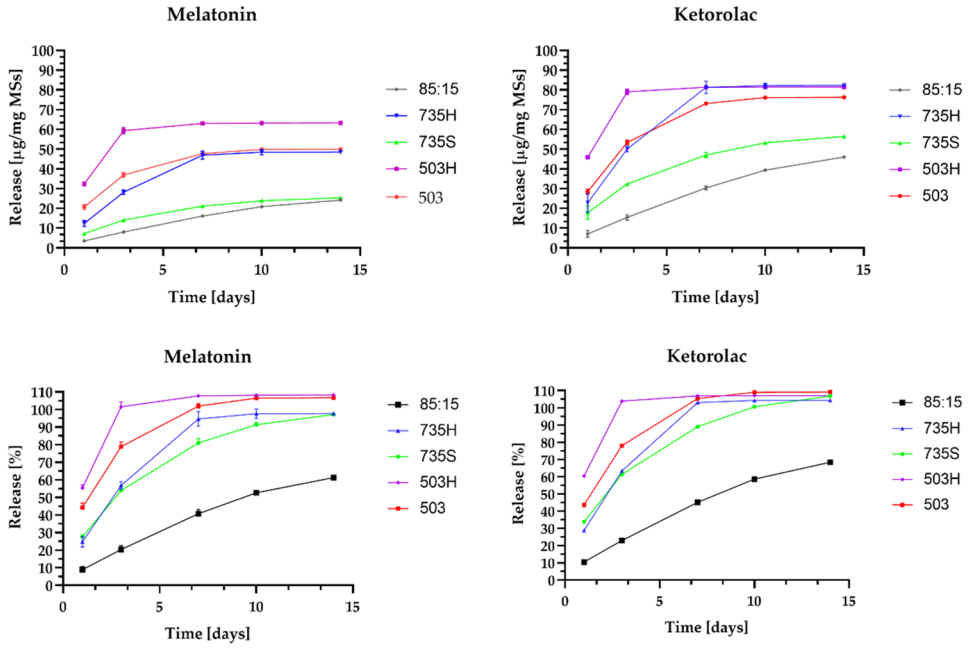

Figure 2. In vitro release of melatonin and ketorolac in MSs prepared with 80 mg melatonin and 60 mg ketorolac during 14 days in µg/mg MSs and percentage (%).

PLGA 735H, only statistically significant differences with 735S ($p = 0.0005$) and 85:15 ($p = 0.021$) polymers were found.

3.1.2. In vitro release studies

An initial release study over 14 days was performed with MSs loaded with melatonin and ketorolac. As can be seen in figure 2, drugs were completely released during this two-weeks period except for MSs prepared from PLGA 85:15, which released 61.27 ± 0.63% of the melatonin and 68.43 ± 0.18% of the loaded ketorolac. As expected, PLGA 503 and 503H, both with a lactic acid - glycolic acid ratio of 50:50, showed a faster release of the drugs, while the polymers 735 S and 735 H, with a ratio of 75:25, showed a slower, but still high release in this period.

Polymers with a 50:50 ratio of lactic-glycolic acid had the highest burst release, being 44.22 ± 2.63% for melatonin and 43.65 ± 1.91% for ketorolac in the case of PLGA 503 polymer and 55.37 ± 1.79% for melatonin and 60.37 ± 1.20% for ketorolac when PLGA 503H polymer was used. As previously described, the difference observed between PLGA 503 and 503H is probably due to the higher hydrophilicity of 503H (Park *et al.* 2018, Nieto *et al.* 2020). The 75:25 ratio PLGAs showed also high burst values, being 27.62 ± 1.24% for melatonin and 33.90 ± 6.58% for ketorolac in the case of 735S and 24.86 ± 2.93% and 28.86 ± 5.99% for melatonin and ketorolac respectively for 735H.

Burst results for PLGA 85:15, with 8.91 ± 1.74% for melatonin and 10.51 ± 2.50% for ketorolac, resulted significantly lower than the initial release observed for MS prepared with all other PLGAs ($p < 0.05$).

According to the results obtained, the polymer PLGA 85:15 was selected for further technological development of the melatonin, ketorolac, and latanoprost tri-loaded microspheres.

Table 2. Mean size of melatonin and ketorolac microspheres developed with PLGA 85:15 with and without vitamin E expressed in µm ± SD.

Formulation	Particle size (µm ± SD)
KM	30.04 ± 6.51
KMVE	32.35 ± 8.64

Table 3. Mean size of ketorolac, melatonin and latanoprost microspheres developed with PLGA 85:15 expressed in µm ± SD.

Formulation	Particle size (µm ± SD)
KML	28.86 ± 5.14
KMLVE	33.58 ± 5.44

3.2. Technological development of multi-loaded formulations

After selection of PLGA 85:15 as the polymer with the most appropriate properties for the controlled release of melatonin and ketorolac, the inclusion of latanoprost and vitamin E as an oily additive in the MSs was performed.

3.2.1. Microspheres characterization

3.2.1.1. Size and morphology. Addition of vitamin and/or latanoprost did not modify the average particle sizes of MSs developed with PLGA 85:15 (Tables 2 and 3) ($p > 0.05$).

All formulations resulted in spherical shape (Figure 3). While particle prepared without vitamin E offered smooth surfaces (independently on the drug/s content), MSs containing vitamin E in their composition (KMVE and KMLVE) showed small surficial pores.

To confirm that vitamin E caused the presence of pores in the MSs, visualization of blank PLGA 85:15 MSs, without (Blank MSs) and with the addition of vitamin E (Blank MSs VE), was also performed (Figure 4).

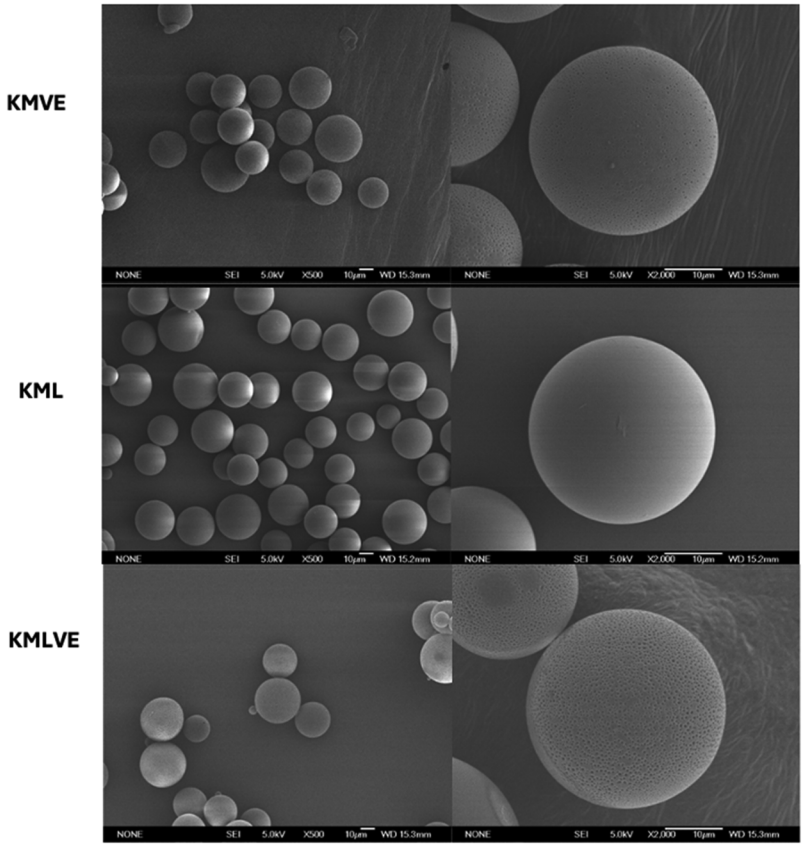

Figure 3. Microspheres prepared with melatonin, ketorolac, and latanoprost developed with PLGA 85:15 (with and without vitamin E) visualized by scanning electron microscopy.

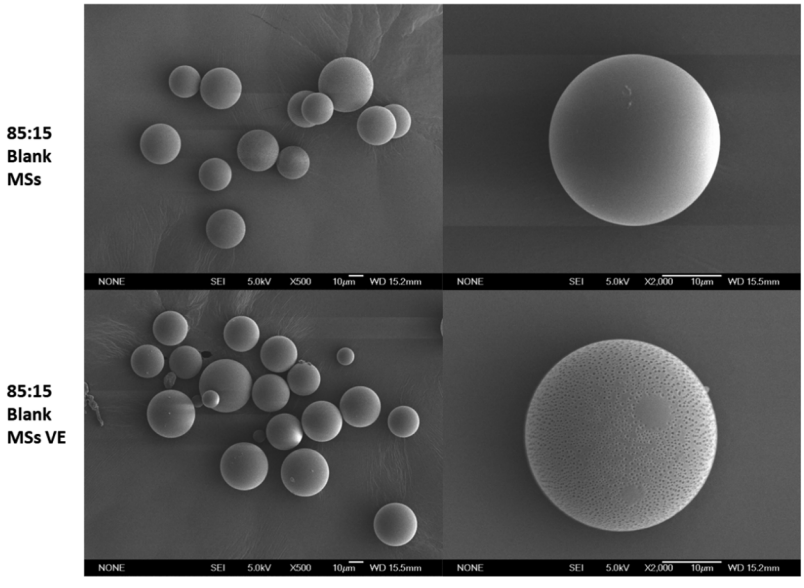

Figure 4. Blank microspheres (with and without vit E addition) developed with PLGA 85:15 visualized by scanning electron microscopy.

3.2.1.2. Encapsulation efficiency. Inclusion of vitamin E did not affect encapsulation efficiency of ketorolac ($p > 0.05$. Although slightly less encapsulation was observed for melatonin with the inclusion of vitamin E in the formulation (Table 4), the results were not statistically significant ($p = 0.13$).

The latanoprost EE resulted approximately 100%, according to its high affinity for the oily phase due to its low water solubility (Horne *et al.* 2017). The inclusion of latanoprost in the formulation did not modify the content of ketorolac and melatonin (Table 5).

In addition, there were no significant differences between the EE (%) of the three active substances (melatonin, ketorolac and latanoprost) due to vitamin E addition ($p > 0.05$ for all combinations).

Table 4. Encapsulation efficiency (EE) in µg/mg Mss and % of melatonin and ketorolac in MSs developed with 85:15 PLGA polymer with and without vitamin E addition (mean ± SD).

	EE [µg/mg ms]		EE [%]	
Formulation	Melatonin	Ketorolac	Melatonin	Ketorolac
KM	39.55 ± 3.15	67.24 ± 5.32	26.68 ± 2.11	60.46 ± 4.67
KMVE	29.23 ± 8.93	65.63 ± 7.73	20.09 ± 6.54	62.61 ± 2.40

Table 5. Encapsulation efficiency (EE) in µg/mg MSs and % of melatonin (Mel), ketorolac (Ket) and latanoprost (Lat) in MSs developed with 85:15 polymer with and without vitamin E addition (mean ± SD).

	EE [µg/mg MSs]			EE [%]		
Formulation	Melatonin	Ketorolac	Latanoprost	Melatonin	Ketorolac	Latanoprost
KML	38.44 ± 11.10	76.78 ± 10.38	8.12 ± 1.13	25.85 ± 7.49	69.42 ± 9.32	109.89 ± 5.30
KMLVE	39.70 ± 5.89	67.28 ± 4.17	7.51 ± 0.58	26.81 ± 3.98	59.87 ± 5.08	101.98 ± 7.80

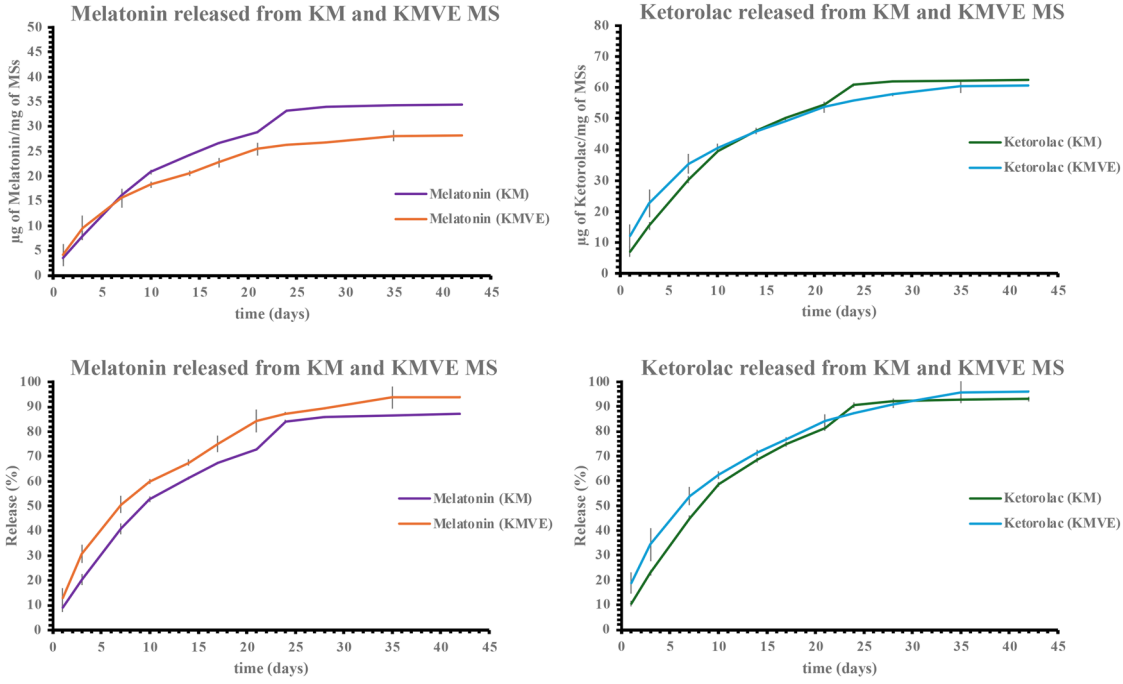

Figure 5. In vitro release in µg/mg MSs (up) and % (down) of melatonin and ketorolac in PLGA 85:15 MSs prepared with 80 mg melatonin and 60 mg ketorolac with and without vitamin E for 42 days.

3.2.2. In vitro release studies

Initially, and to evaluate the possible influence of vitamin E in the release of melatonin and ketorolac in MSs fabricated with PLGA 85:15, a 42 days (6 weeks) in vitro release study was performed without and with addition of the oily additive (KM and KMVE respectively) (Figure 5).

The similarity factor was used to compare the different in vitro release obtained (Javier *et al.* 2021). The results showed similarity when comparing melatonin (f2 = 65.13) and ketorolac (f2 = 70.12) profiles.

In the subsequent step of the optimization process, latanoprost was included in the formulations. It is worth mentioning that the formulations with vitamin E were preferred due to its antioxidant properties and because the addition of the oily substance would help encapsulating proteins in its solid state in PLGA MSs if needed [30]. The use of this technological results has been previously developed in the research group [31].

The release studies of KMLVE MSs were carried out for 70 days (10 weeks) (Figures 6 and 7) with 62.71 ± 0.40% of the encapsulated latanoprost released by that time, indicating a controlled release that could last for several months (Figure 9).

According to the previous in vitro characterization, KMLVE formulation was selected for the in vivo studies, due to the higher encapsulation of latanoprost, without affecting the controlled release of the other active ingredients.

In addition, to check the homogeneity between batches, the release profiles of 4 different batches (KMLVE-1, KMLVE-2, KMLVE-3, and KMLVE-4) were compared. Once demonstrated similarity between them, the batches were mixed to form a pool, whose sustained release was also studied and compared with the separated batches KMLVE1-4 (Figure 8).

3.3. In vitro cell assays

3.3.1. Cytotoxicity assay

The cell viability of all formulations (blank, single loaded and co-loaded with and without vitamin E addition) in the assayed conditions resulted above 90%, showing good tolerance in retinal cells (Figure 9) without significant differences

between them. The cell viability results for the microspheres were 94.63 ± 6.21 for MSs B, 91.36 ± 3.64% for MSs B VE, 90.46 ± 2.92% for MSs-Ketorolac, 93.76 ± 2.34% MSs-Melatonin and 99.42 ± 7.36% for MSs-Latanoprost. When ketorolac and melatonin were combined, the results resulted 90.77 ± 3.71% and 92.71 ± 0.84% of cell viability for KM and KMVE respectively. In the case of the tri-loaded MSs with different amounts of latanoprost the value resulted 96.04 ± 0.97% for KMLVE.

3.4. In vivo ophthalmological evaluation

Intravitreal treatment was well tolerated, nor red eye neither evident infection nor inflammation was detected.

3.4.1. Intraocular pressure

The cohort of animals with induced glaucoma developed a slowly progressive increase in IOP reaching ocular hypertension values at 10th week of follow-up onwards. The cohort of glaucomatous animals with intravitreal treatment KMLVE presented an early ocular hypertensive peak (22.33 ± 5.86 mmHg) at week 6 (4 weeks followed the first intravitreal injection), but subsequently decreased progressively until reaching the lowest final value (Control: 19.00 ± 4.28 vs Glaucoma: 22.96 ± 2.51 vs Glaucoma + IV treatment KMLVE: 16.27 ± 2.93 mmHg, pANOVA = 0.005) (Figure 10A). Bilaterality sub-analysis showed that both eyes in the glaucoma cohort treated with the intravitreal treatment KMLVE developed a similar IOP increase, even when only the right eye was injected, until week 6 (hypertensive peak), thereafter the IOP of the treated right eyes decreased progressively and significantly at week 12 -with one IV- (21.13 ± 2.98 vs 24.04 ± 3.06 mmHg; $p < 0.05$) and more accentuated at week 24 -after two IV- (16.27 ± 2.93 vs 21.87 ± 2.25 mmHg, $p = 0.010$) compared to left eyes that maintained with ocular hypertensive levels (Figure 10B). Sub-analysis by sex revealed that glaucomatous males treated with the intravitreal treatment KMLVE (19.54 ± 4.09 vs 16.03 ± 3.29 mmHg; $p < 0.05$), presented higher IOP levels compared to females. However, intravitreal treatment resulted in a similar decrease in IOP in both sexes (Figure 10C).

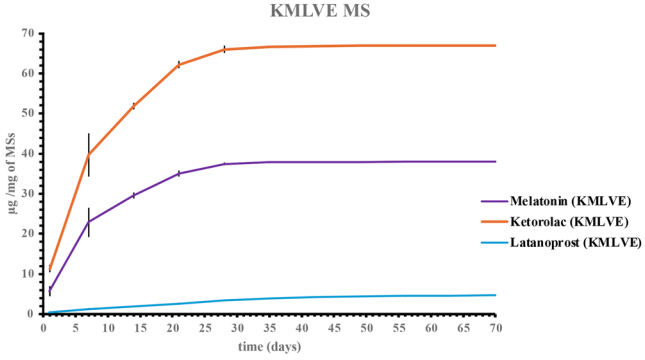

Figure 6. Melatonin, ketorolac and latanoprost in vitro release from KMLVE MSs expressed in µg of loaded compounds/mg of MSs and in % released.

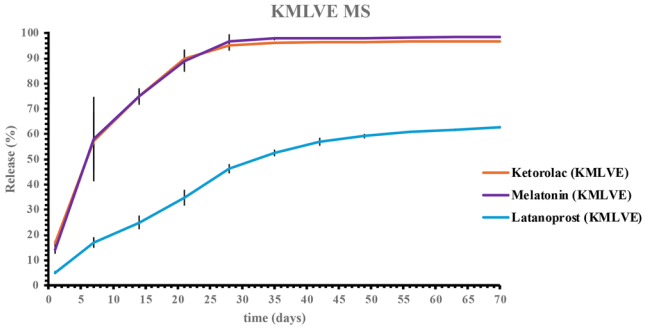

Figure 7. Melatonin, ketorolac and latanoprost in vitro release from KMLVE MSs expressed in percentage (%) of drug released.

3.4.2. Electroretinography

To evaluate the functional protective effect of the intravitreal treatment KMLVE on neuroretina, the three cohorts were compared. In the Scotopic ERG test: The cohort with Glaucoma + IV treatment KMLVE showed the shortest latencies in bipolar cells (bms: steps 1, 3, 4, 5, and 6; $p < 0.05$), at week 12. However, the trend is reversed, and it showed longer latencies in bipolar cells (bms: steps 3, 4 and 5; $p < 0.05$) at week 24. The Control cohort of healthy animals showed greater bipolar amplitude than the Glaucoma + IV treatment KMLVE cohort and the Glaucoma cohort ($p < 0.05$) at week 12 and maintained in bipolar and photoreceptors ($p < 0.05$) at week 24. Interestingly, the Glaucoma + IV treatment KMLVE cohort increased amplitude compared to the Glaucoma cohort throughout the study. In the Photopic Negative Response test: The Glaucoma + IV treatment KMLVE cohort showed higher bipolar and similar RGC amplitudes than the healthy animals (Control > Glaucoma + IV treatment KMLVE > Glaucoma) (PhNRwave: 34.73 ± 22.32 vs 32.57 ± 27.58 vs 8.28 ± 6.87 mV; $p = 0.283$) at week 12. Interestingly, the Glaucoma + IV treatment KMLVE cohort showed a trend of functional improvement, with shorter latencies and greater PhNR amplitude (Glaucoma + IV treatment KMLVE > Control > Glaucoma) (PhNRwave: 22.02 ± 18.07 vs 11.75 ± 11.94 vs 5.66 ± 4.57 mV; $p = 0.126$), at week 24 (Table 6). In the cohort treated, a sub-analysis of bilaterality comparing right eyes

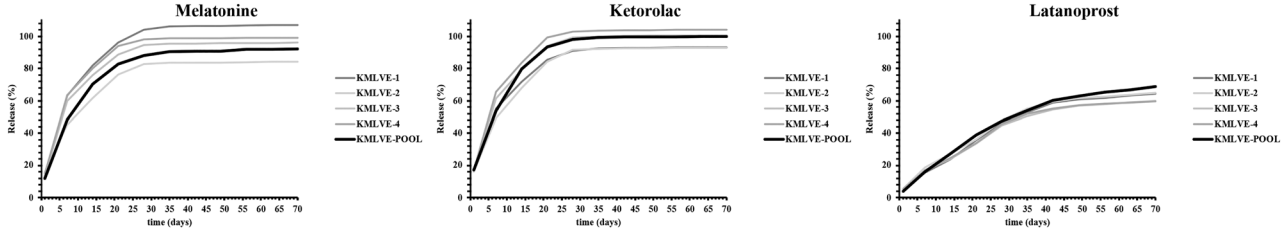

Figure 8. In vitro release in percentage (%) of melatonin, ketorolac and latanoprost in KMLVE1-4 MSs batches.

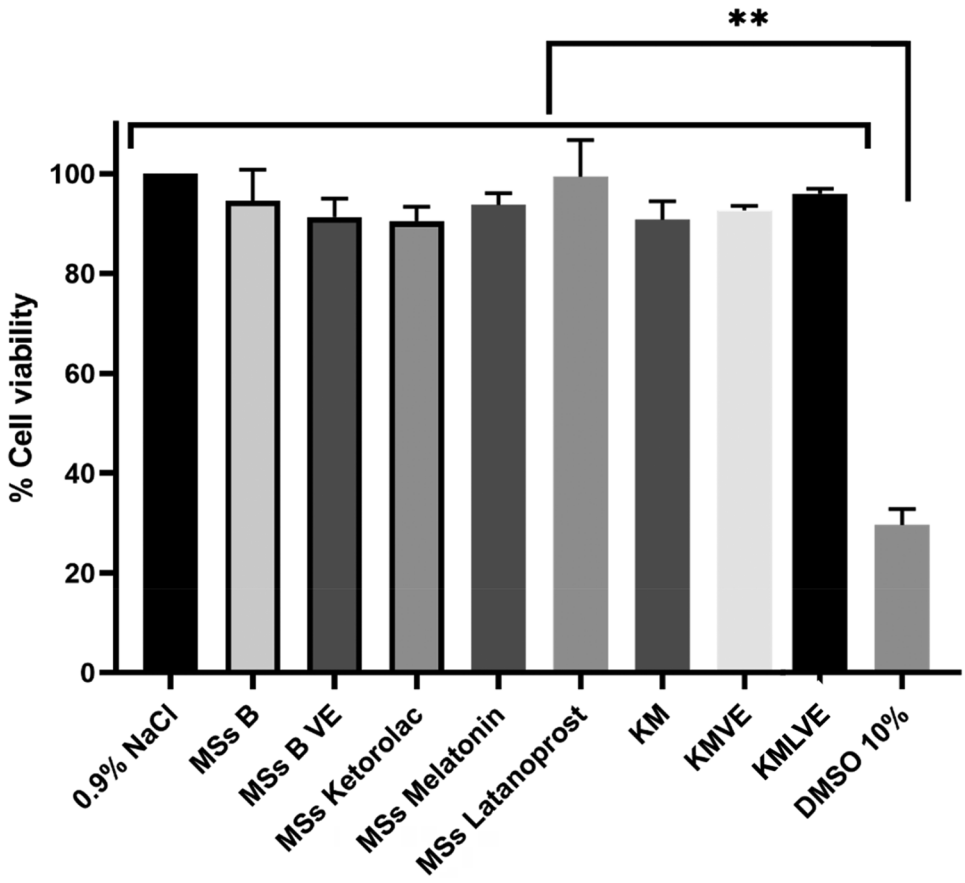

Figure 9. Cell viability evaluation of PLGA 85:15 microspheres formulations containing different active substances. $^{**}p < 0.001$.

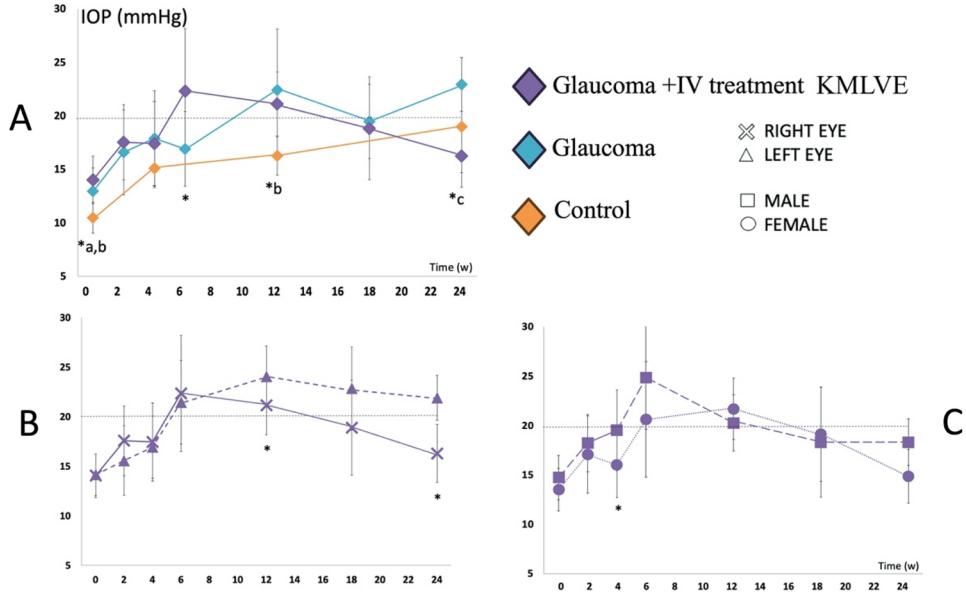

Figure 10. Intraocular pressure (IOP). Comparison of intraocular pressure curves in the three cohorts (a). Subanalysis by eye laterality (B) and by sex (C) in the treated cohort. G: Glaucoma cohort; IV: intravitreal injection. *: statistical significance ($p < 0.05$), a: differences between healthy control and glaucoma treated, b: differences between healthy control and glaucoma, c: differences between glaucoma and glaucoma treated.

(glaucoma-induced and treated) to their contralateral left eye (non-intervened) showed that right eyes still presented a trend of longer latencies and lower amplitude in photoreceptor (a wave: steps 1 and 7; $p < 0.05$) and bipolar cells (b wave: steps 2, 3 and 4; $p < 0.05$) at week 24 (Figure 11A). Although, in the PhNR test right eyes presented better functionality in photoreceptor cells at week 12 but worse at 24 weeks, and in bipolar and RGCs and over the study ($p < 0.05$) (Figure 11B). Finally, to ascertain whether the IV treatment KMLVE was more effective in males or females, a sex sub-analysis

Table 6. Electroretinography (ERG). Comparison of electroretinography response in the three cohorts. IV: intravitreal injection. Statistical significance ($p < 0.05$), a: differences between healthy control and glaucoma treated, b: differences between healthy control and glaucoma, c: differences between glaucoma and glaucoma treated.

ERG PARAMETERS Right eye Both sexes		12 w				24 w			
		CONTROL Mean ± SD	Glaucoma Mean ± SD	Glaucoma + IV KMLVE Mean ± SD	Sig. ANOVA	CONTROL Mean ± SD	Glaucoma Mean ± SD	Glaucoma + IV KMLVE Mean ± SD	Sig. ANOVA
Step 1	**a_[ms]**	18.50 ± 8.04	19.67 ± 6.69	17.48 ± 9.40	0.934	19.87 ± 8.24	13.30 ± 6.06	19.32 ± 8.11	0.316
	b_[ms]	41.36 ± 9.75	65.50 ± 7.13	31.08 ± 13.61	**0.004** b=0.043, c=0.004	34.82 ± 21.38	26.86 ± 19.54	40.56 ± 24.92	0.567
	a-wave_[μV]	28.27 ± 28.46	2.65 ± 1.71	15.58 ± 11.98	0.218	16.87 ± 14.75	13.02 ± 13.37	23.64 ± 16.26	0.438
	b-wave_[μV]	75.12 ± 29.77	19.63 ± 6.68	47.12 ± 26.09	**0.034** b=0.037	30.99 ± 17.72	32.02 ± 28.60	31.34 ± 21.69	0.997
Step 2	**a_[ms]**	17.26 ± 8.01	22.37 ± 10.72	20.57 ± 4.56	0.610	20.90 ± 8.70	17.56 ± 7.97	21.22 ± 7.49	0.696
	b_[ms]	65.20 ± 23.54	71.20 ± 0.00	46.68 ± 8.12	0.074	78.18 ± 12.50	70.24 ± 2.14	70.16 ± 1.35	0.088
	a-wave_[μV]	49.96 ± 24.65	12.00 ± 16.29	29.93 ± 23.76	0.113	15.60 ± 9.22	8.20 ± 3.39	17.18 ± 12.19	0.278
	b-wave_[μV]	396.02 ± 241.93	158.30 ± 132.71	103.47 ± 33.58	**0.029** a=0.034	498.17 ± 264.41	210.60 ± 94.85	309.37 ± 114.80	**0.033** b=0.040
Step 3	**a_[ms]**	20.16 ± 10.34	26.70 ± 4.27	22.62 ± 4.46	0.481	20.55 ± 6.14	22.88 ± 6.21	25.64 ± 5.29	0.267
	b_[ms]	52.34 ± 7.28	69.87 ± 1.15	47.48 ± 2.31	**0.000** b=0.001, c=0.000	49.32 ± 19.05	66.14 ± 5.46	67.04 ± 4.42	**0.017** a=0.025
	a-wave_[μV]	89.62 ± 60.69	51.60 ± 39.19	30.78 ± 26.86	0.132	42.17 ± 29.08	43.87 ± 31.92	64.71 ± 41.47	0.422
	b-wave_[μV]	193.20 ± 86.60	110.03 ± 60.75	101.18 ± 31.36	0.074	151.15 ± 75.85	157.60 ± 56.72	206.36 ± 46.29	0.170
Step 4	**a_[ms]**	21.10 ± 5.90	23.27 ± 2.75	15.42 ± 3.48	0.052	21.47 ± 6.34	20.82 ± 2.95	20.09 ± 5.56	0.886
	b_[ms]	53.00 ± 6.52	68.23 ± 4.54	49.08 ± 1.92	**0.000** a=0.003, c=0.000	56.38 ± 5.05	66.42 ± 7.09	68.10 ± 4.01	**0.001** b=0.018, a=0.002
	a-wave_[μV]	78.44 ± 47.27	13.52 ± 7.33	52.35 ± 28.98	0.076	34.50 ± 20.79	28.05 ± 19.95	21.69 ± 12.40	0.383
	b-wave_[μV]	521.80 ± 240.14	269.00 ± 143.51	351.68 ± 49.37	0.111	550.83 ± 173.73	346.80 ± 136.23	483.66 ± 131.38	0.094
Step 5	**a_[ms]**	21.22 ± 2.40	19.83 ± 1.15	21.47 ± 1.87	0.511	20.22 ± 2.07	18.64 ± 0.31	19.80 ± 0.84	0.137
	b_[ms]	49.32 ± 2.38	62.57 ± 7.03	48.85 ± 1.66	**0.000** b=0.00, a=0.001	54.33 ± 5.45	60.56 ± 6.00	65.37 ± 4.50	**0.003** a=0.003
	a-wave_[μV]	107.20 ± 70.32	84.77 ± 84.04	76.75 ± 29.09	0.695	182.67 ± 89.42	86.02 ± 28.63	96.19 ± 43.34	**0.019** b=0.046, a=0.040
	b-wave_[μV]	559.00 ± 266.58	388.00 ± 220.02	415.90 ± 49.28	0.377	731.50 ± 316.56	412.20 ± 147.47	542.17 ± 156.12	0.070
Step 6	**a_[ms]**	15.34 ± 2.40	15.97 ± 3.25	13.12 ± 1.56	0.170	14.03 ± 1.42	13.98 ± 3.35	16.04 ± 1.84	0.151
	b_[ms]	46.32 ± 3.63	57.33 ± 3.25	48.17 ± 2.52	**0.001** b=0.002, c=0.005	52.52 ± 7.05	58.92 ± 6.11	58.29 ± 6.51	0.203
	a-wave_[μV]	213.30 ± 136.79	147.23 ± 102.43	173.48 ± 20.83	0.618	239.83 ± 95.17	156.36 ± 64.57	154.63 ± 65.22	0.099
	b-wave_[μV]	604.60 ± 269.96	436.67 ± 213.95	492.45 ± 77.81	0.468	728.17 ± 348.90	464.40 ± 170.85	507.92 ± 163.64	0.145
Step 7	**a_[ms]**	19.58 ± 8.74	21.00 ± 4.81	19.40 ± 6.75	0.949	23.62 ± 8.90	20.16 ± 4.11	21.53 ± 8.24	0.755
	b_[ms]	25.36 ± 13.17	47.97 ± 9.88	35.62 ± 14.10	0.102	41.90 ± 15.01	52.32 ± 19.65	38.73 ± 18.74	0.411
	a-wave_[μV]	68.51 ± 53.54	15.10 ± 13.28	59.33 ± 76.47	0.486	21.18 ± 24.60	29.23 ± 39.41	26.40 ± 22.33	0.887
	b-wave_[μV]	100.59 ± 77.07	43.10 ± 17.49	82.85 ± 85.39	0.584	50.92 ± 22.58	90.34 ± 55.83	50.09 ± 34.15	0.155
PhNR	**a_[ms]**	13.80 ± 3.75	12.60 ± 3.36	17.18 ± 7.02	0.436	16.03 ± 6.36	13.52 ± 5.62	17.06 ± 5.29	0.549
	b_[ms]	28.48 ± 15.27	39.13 ± 7.74	30.23 ± 14.52	0.566	28.02 ± 14.34	27.30 ± 13.62	26.30 ± 11.65	0.968
	PhNR_[ms]	42.72 ± 8.06	44.30 ± 8.68	43.15 ± 7.68	0.964	45.25 ± 3.14	46.10 ± 2.59	42.24 ± 4.93	0.188
	a-wave_[μV]	20.06 ± 18.96	2.15 ± 3.68	24.82 ± 16.04	0.168	24.66 ± 7.96	14.83 ± 10.98	19.00 ± 16.13	0.587
	b-wave_[μV]	20.05 ± 12.53	20.13 ± 4.66	32.97 ± 22.87	0.415	24.85 ± 9.05	39.52 ± 23.65	28.16 ± 16.53	0.346
	PhNR_[μV]	34.73 ± 22.32	8.28 ± 6.87	32.57 ± 27.58	0.283	11.75 ± 11.94	5.66 ± 4.57	22.02 ± 18.07	0.126

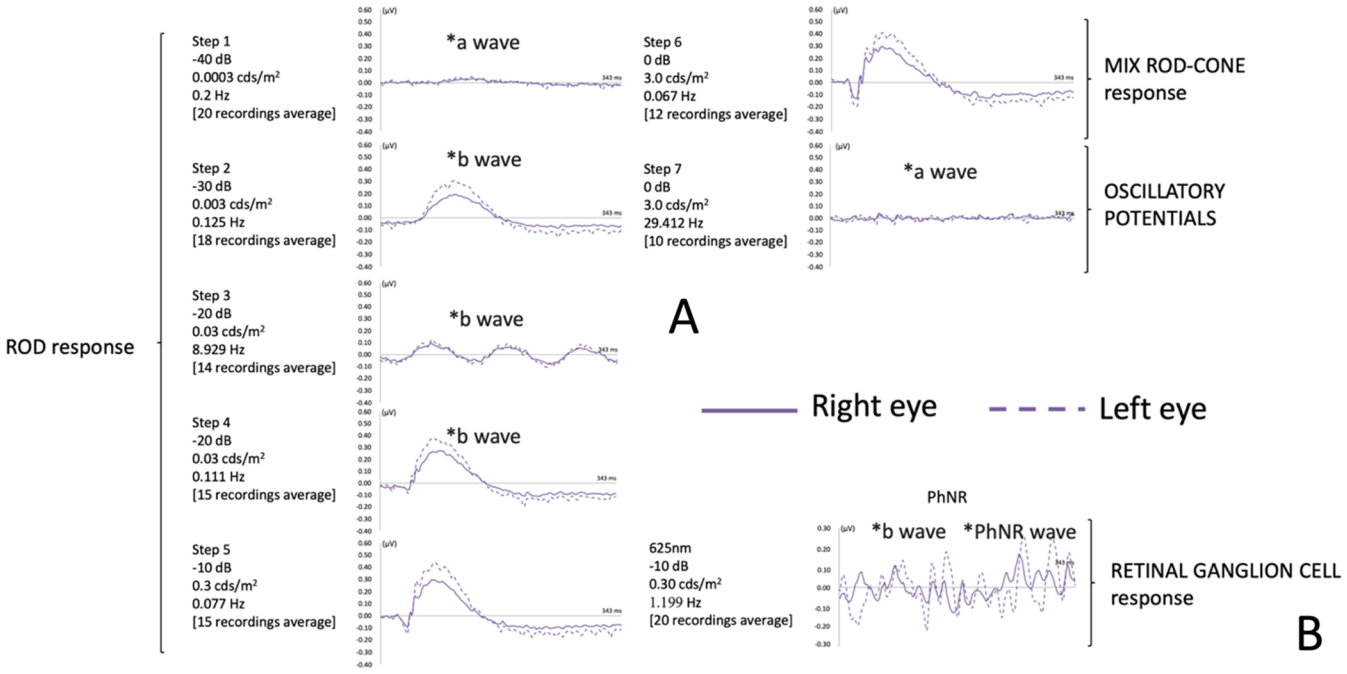

Figure 11. Neuroretinal functionality measured by electroretinography in the glaucoma + IV treatment KMLVE at 24 weeks of follow-up. A sub-analysis of bilaterality comparing right eyes (glaucoma-induced and treated) to their contralateral left eye (non-intervened).

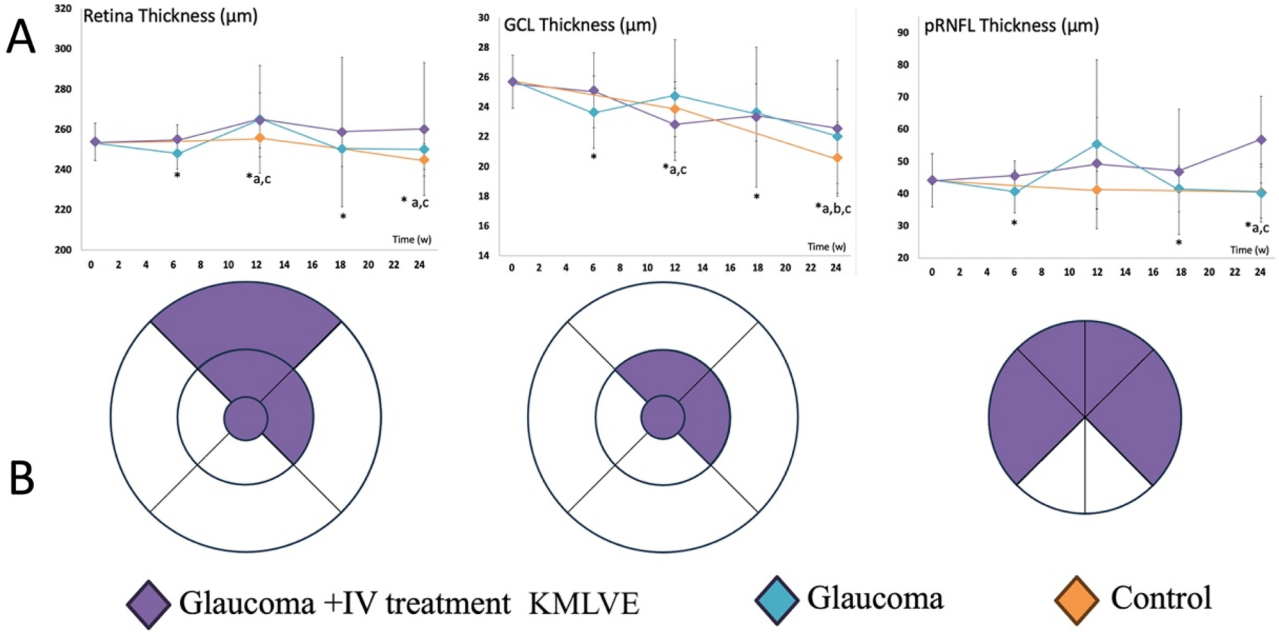

Figure 12. Neuroretinal thickness measured by OCT. A: Comparison of neuroretinal change in the three cohorts over 24 weeks of study. B. Optical coherence tomography sectors with increased thickness in cohort glaucoma + IV treatment KMLVE at the end of the study. *: statistical significance ($p < 0.05$), a: differences between healthy control and glaucoma treated, b: differences between healthy control and glaucoma, c: differences between glaucoma and glaucoma treated.

was performed, which found no differences ($p > 0.05$) between sexes in neuroretinal functionality over the study.

3.4.3. Optical coherence tomography

Comparing the three cohorts with each other, the Glaucoma + IV treatment KMLVE cohort showed greater thickness compared to the Glaucoma cohort and the Control cohort, in the GCL (central sector) and in the RNFL (temporal and superior temporal sectors) ($p < 0.05$: sectors marked in purple in Figure 12) at week 18; and in the retina (central, inner-nasal, inner-superior and outer-superior sectors; $p < 0.05$), in the GCL (central, inner-nasal and inner-superior sectors; $p < 0.05$) and in the RNFL (temporal, temporal-superior, nasal and nasal-superior sectors; $p < 0.05$) at week 24 (Figure 12). When specifically analyzing the Glaucoma + IV treatment KMLVE cohort (Figure 13), the treated right eyes, compared to left eyes, showed a trend of lower thickness in GCL (central sector; $p < 0.05$) until week 12; but then reversed with greater thickness in Retina (outer-inferior sector; $p < 0.05$) at week 18, and in Retina (inner-nasal and inner-superior

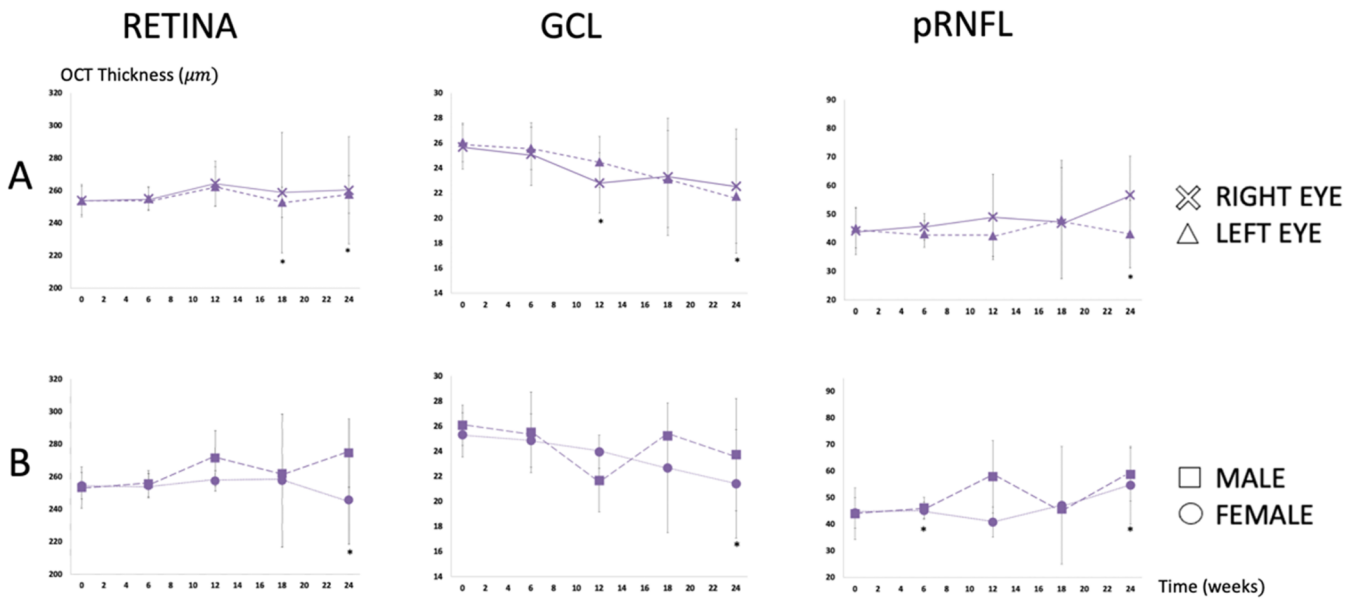

Figure 13. Neuroretinal thickness measured by OCT in the cohort with glaucoma and intravitreal treatment KMLVE. (A) Subanalysis by eye laterality (B) and by sex. *: statistical significance ($p < 0.05$).

sectors), GCL (inner-superior sector) and RNFL (temporal sector) (all $p < 0.05$) at week 24 (Figure 13A). Both sexes of the Glaucoma + IV treatment KMLVE cohort presented greater thickness, compared to the rest of the cohorts, in the retina (males in the inner and outer-nasal sectors, and females in the inner-nasal and inner-superior sectors; all $p < 0.05$), and in the GCL (males in the central sector and females in the central, inner-nasal and inner-superior sectors, all $p < 0.05$) at week 24. However, only males presented greater RNFL thickness (nasal and nasal-inferior sectors; $p < 0.05$) at week 12, and (temporal and temporal-superior sectors; $p < 0.05$) at week 24. So, when assessing whether there were differences by sex, the males treated showed greater thickness compared to females in RNFL (temporal and temporal-superior sectors) at week 6, (nasal-inferior sector) at week 12, and (temporal sector) at week 24, and in the retina (inner-inferior sector) at week 24 (all $p < 0.05$) (Figure 13B).

3.4.4. Histological assessment

To evaluate the effect of the treatment in neuroretinal populations, RGCs morphometric analysis was performed in retinal sections from Healthy, Glaucoma and KMLVE- treated rats 12 and 24 weeks after glaucoma induction. No overt loss of RGC was observed in the Glaucoma cohort when compared with Healthy rats at both time points, with no significant changes after treatment (Figures 14 and 15, left panel). Interestingly, Glaucoma rats showed a significant increase in GFAP immunopositivity 24 weeks after glaucoma induction (Figure 15, right panel), indicating the presence of astrogliosis. Muller cells processes were also GFAP positive, as a consequence of this reactive status of glial cells. These alterations were less consistently observed at 12 weeks after glaucoma induction (Figure 14, right panel), suggesting progressive, cumulative damage in the glaucomatous retinas. After KMLVE treatment, GFAP values were normalized 24 weeks after the induction of glaucoma (Figure 15, right panel).

4. Discussion

Since glaucoma is a multifactorial neurodegenerative disease, an interesting strategy consists of the treatment combining neuroprotective active substances with different mechanisms of action and capable of approaching the therapy from different pathways involved in its pathophysiology. As the retina is the target site of neuroprotective drugs in glaucoma, intravitreal administration allows to effectively reach intraocular tissues. However, frequent injections are needed to maintain therapeutic concentrations in the posterior ocular tissues. If the medication is formulated in an IODDS, the adverse effects associated with repeated intravitreal injections would be reduced.

In this sense, in recent years, authors have studied the inclusion of different kinds of neuroprotective substances in PLGA microspheres intended for glaucoma treatment by intraocular administration (Arranz-romera *et al.* 2019, Arranz-Romera *et al.* 2021). Among the drugs with neuroprotective potential, we highlight two compounds: melatonin and ketorolac. Melatonin is an antioxidant active ingredient with demonstrated neuroprotective activity (Belforte *et al.* 2010, Reiter *et al.* 2016, Bessone *et al.* 2019), which also has shown an effect on lowering intraocular pressure in other studies (Saniples *et al.* 2000, Lee and Goldberg 2011). On the other hand, the inclusion of anti-inflammatory drugs in controlled release systems based on PLGA microspheres for glaucoma treatment is increasingly being investigated (Jiang *et al.* 2007, Mietzner *et al.* 2020). PLGA microspheres have been studied to encapsulate anti-inflammatory active ingredients in numerous studies (Bravo-osuna *et al.* 2018). Among the most frequently used anti-inflammatories in intraocular controlled release systems are, for example, dexamethasone (Pan *et al.* 2020, Brugnera *et al.* 2022) and the employed in this work ketorolac, which has managed to be released for 50 days when encapsulated in PLGA microspheres (Nadal-Nicolás *et al.* 2016). Moreover, ketorolac has also been shown in

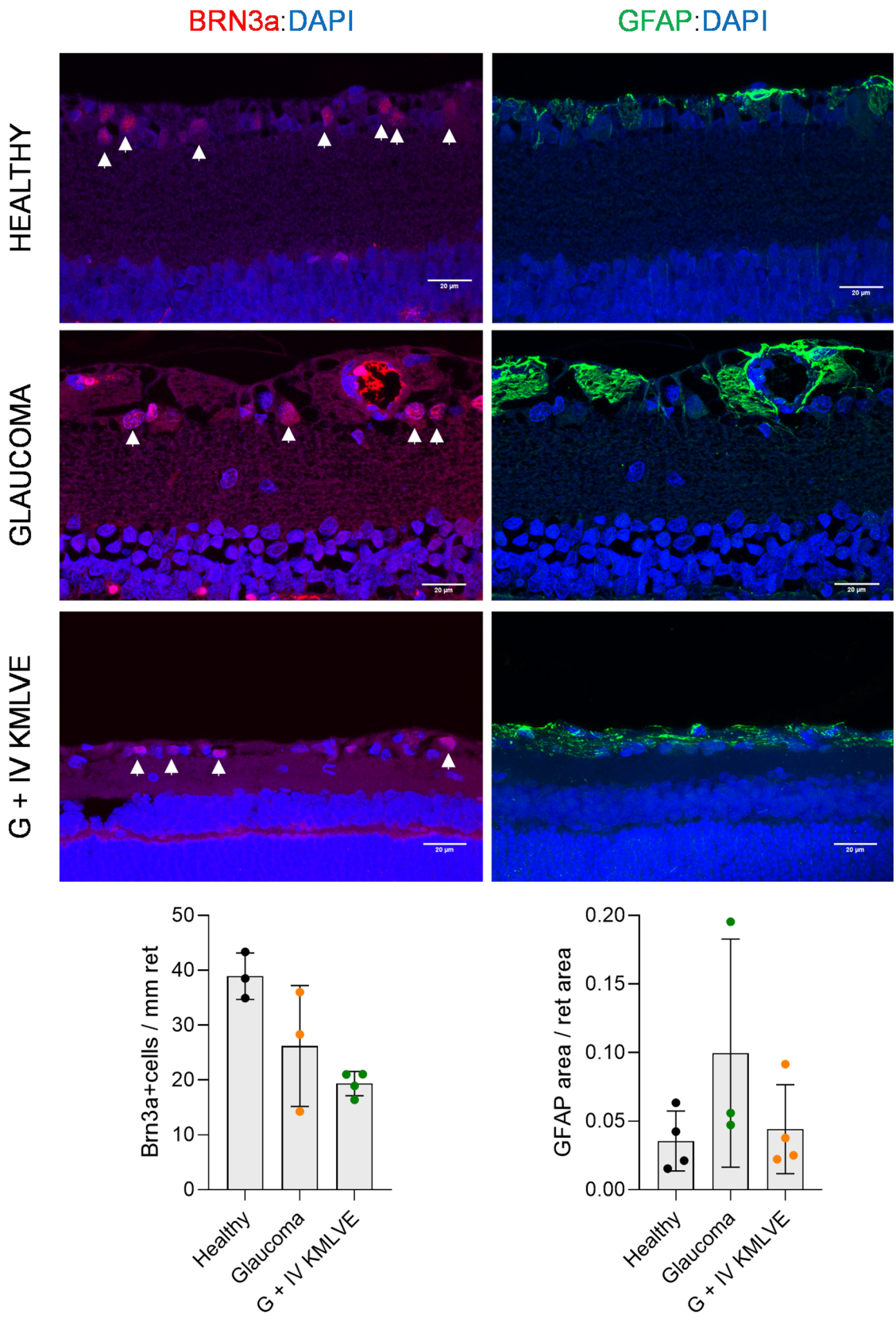

Figure 14. Histological assessment of retinal sections of healthy, glaucoma and intravitreal treatment KMLVE 12 weeks after glaucoma induction. Brn3a immunostaining for RGC detection (left panel) and GFAP immunostaining for gliosis evaluation (right panel). *: statistical significance ($p < 0.05$).

previous studies to enhance IOP reduction in combination with latanoprost (Turan-Vural *et al.* 2012).

Furthermore, the study of the inclusion of active ingredients capable of reducing IOP in controlled-release systems is also increasing. This is the case of DURYSTA, an intracameral implant of the hypotensive bimatoprost, which has recently received FDA approval (Shirley 2020, Sirinek *et al.* 2022). In this sense, as pointed out in the introduction,

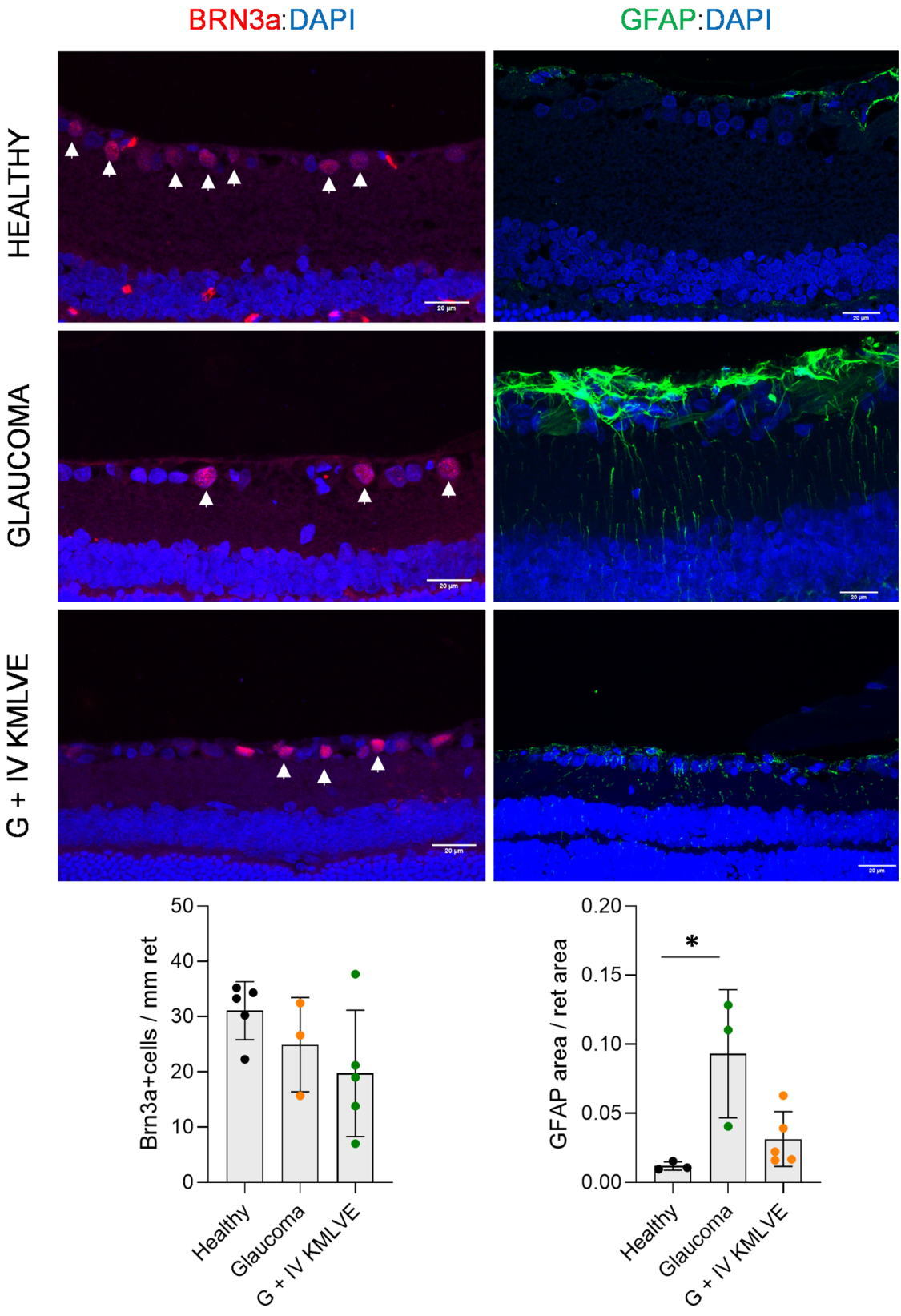

Figure 15. Histological assessment of retinal sections of healthy, glaucoma and intravitreal treatment KMLVE 24 weeks after glaucoma induction. Brn3a immunostaining for RGC detection (left panel) and GFAP immunostaining for gliosis evaluation (right panel). *: statistical significance ($p < 0.05$).

latanoprost is used in clinics as hypotensive drug in eye drops for glaucoma patients, and in addition it has been observed also inherent neuroprotective activity for this compound.

For all these reasons, in this work it was decided to combine the three mentioned compounds (ketorolac, melatonin and latanoprost) in the same PLGA microspheres to address glaucoma from intraocular hypotension and neuroprotection

perspectives. During the design of this piece of research, the amount of both ketorolac and melatonin included in the polymer matrix was selected based on previously published studies and recent improvements to the protocol. As neurodegeneration occurs through different pathways, we have tried to demonstrate that the combination of these low-molecular-weight drugs, including latanoprost, in the same device, may result effective (Nadal-Nicolás *et al.* 2016, García-Caballero *et al.* 2018, Arranz-romera *et al.* 2019).

Initial studies of the technological development of the tri-loaded MSs consisted of the selection of the most appropriate type of PLGA to develop the formulation. The MSs initially included only melatonin and ketorolac, to later study the addition of vitamin E as an oily additive and latanoprost. Within the PLGAs studied, two had a L-G ratio of 50:50 (503 and 503H), two of 75:25 (753S and 753H) and one of 85:15. Also, two of them had a terminal carboxylic group (503H and 753H). In all cases, the resulting MSs had a similar size (around 30 µm) and were spherical when visualized by SEM. Our results also agree with previously developed studies with PLGA of different ratios, showing that when the PLGA ratio has a higher proportion of lactic acid, the release is more sustained (Makadia and Siegel 2011). In addition, it can be observed how the presence of carboxylic terminal groups in the PLGA produces an increase in the initial burst. This is in concordance with several studies carried out with PLGA, and is due to the fact that the presence of these carboxylic groups accelerates the hydrolysis of PLGA (Makadia and Siegel 2011, Park *et al.* 2018).

According to the results, although PLGA 85:15 was not the polymer that managed to encapsulate the higher amount of melatonin and ketorolac (39.55 ± 3.15 µg/mg MSs and 67.24 ± 5.32 µg/mg MSs for melatonin and ketorolac respectively), it was the one with which the best sustained release results were obtained, having a significantly lower initial burst than the formulations prepared with the other PLGA evaluated ($p < 0.05$) and being the only one that continued to release ketorolac and melatonin after two weeks of in vitro release (Figure 2). According to the PLGA manufacturer Evonik®, the inherent viscosity of PLGA 503, 503H, 735S and 735 H resulted 0.32 – 0.44 dL/g. However, the inherent viscosity of PLGA 85:15 was 0.55 – 0.75 dL/g and due to its higher molecular weight and different PLA:PGA ratio, may be causes of a slower release (Arrighi *et al.* 2019).

The next technological step was the addition of vitamin E to the formulation. The interest in the inclusion of vitamin E in the MSs was due to its demonstrated antioxidant effect. Furthermore, due to its oily nature, addition of vitamin E is also intended to facilitate the future incorporation of neuroprotective proteins in their solid state, following a well-established microencapsulation protocol developed by our research group (Traber and Atkinson 2007, García-Caballero *et al.* 2017, 2018), which could be useful for future formulations. When the addition of vitamin E to the MSs elaborated with PLGA 85:15 was studied, no significant differences in the encapsulation efficiencies were observed ($p < 0.05$) for the two drugs neither in the release profiles ($f2 > 50$). The in vitro release for both formulations (KM and KMVE) was performed for 42 days, still showing a release of melatonin and ketorolac at the end of the study. The particle sizes obtained were around 30 µm, ideal for intravitreal injection in suspension using common needles. They resulted spherical, with the only peculiarity that small pores were seen on the surface of the MSs containing vitamin E, coinciding with the results presented previously (Checa-Casalengua *et al.* 2011, Arranz-Romera *et al.* 2021). It was explained as a consequence of the slow diffusion of the organic solvent during MSs maturation process due to the concentration of the vitamin in the vicinity of the surface of the microspheres (Checa-Casalengua *et al.* 2011).

The last step in the reported technological development was the inclusion of latanoprost in the formulation. For this study, MSs of PLGA 85:15 with and without vitamin E, and 4 mg of latanoprost were prepared. Again, the MSs obtained were all spherical with a suitable particle size for intravitreal administration in suspension. As expected, the MSs containing vitamin E in their composition presented also small pores on the surface.

The EE (%) of latanoprost was approximately 100% in both cases (KML and KMLVE), which is associated to its lipophilic nature (Horne *et al.* 2017). In addition, the encapsulation efficiencies of melatonin and ketorolac did not differ significantly between the formulations (Table 5). Based on these results, extended in vitro release studies were performed with the KMLVE formulation, due to the previously described advantages. A sustained release of 70 days for ketorolac and melatonin was observed in this long-term in vitro release study. Biodegradable polymeric microdevices control drug release through two primary mechanisms, depending on the polymer's behavior. The first mechanism, known as "heterogeneous degradation," occurs when polymer chains in direct contact with the aqueous medium are progressively hydrolyzed, while those within the matrix remain unaffected. In this case, the microdevice undergoes a "layer-by-layer" erosion, releasing the drug(s) entrapped in these outer layers. The second mechanism, referred to as "homogeneous degradation", involves water penetrating the entire matrix, inducing uniform hydrolysis across all polymer chains. In this process, drug release begins immediately as channels form within the matrix, with release rates increasing as the polymer structure collapses. PLGA micromatrices follow this second mechanism to control drug release (Checa-Casalengua *et al.* 2011, Barbosa-Alfaro *et al.* 2021). These results are promising, since they manage to extend the release for a longer time than previously studies with these two drugs (Nadal-Nicolás *et al.* 2016, Brugnera *et al.* 2022). Regarding latanoprost, only 62.71 ± 0.40% was released in 70 days, indicating a potential release for several months.

The final formulation selected for *in vivo* studies was the one containing vitamin E, that is KMLVE MSs, so it was able to effectively encapsulate and subsequently release the three active compounds in a sustained manner maintaining the in vitro cell viability and leaving the way open for future studies including proteins in the solid state, in addition to offering a potential antioxidant action due to the nature of the oil additive. Additionally, single-drug loaded microspheres were not tested to minimize animal use in accordance with the 3Rs principles, avoid extending the study timeline, and because

their lower protective effects compared to multi-loaded formulations had already been demonstrated in a previous study (Arranz-romera *et al.* 2019).

Regarding the *in vitro* cytotoxicity studies, the microspheres resulted not toxic after a 24-hour exposure to RPE-1 cells, with cell viability greater than 90% being observed in all cases (unloaded and loaded with the drugs individually or as a combination). This is a good indicative of the good ocular tolerance of the microspheres, in agreement with the findings of different authors about the tolerance of PLGA microspheres (Herrero-Vanrell *et al.* 2014, Zhao *et al.* 2017).

This glucocorticoid-induced model mimicked chronic glaucoma in humans, characterized by a progressive increase in intraocular pressure and functional and structural damage to the retina and optic nerve. The combination of functional evaluation through electroretinography, neuroretinal structure assessment using optical coherence tomography, and histological analysis allows for a comprehensive characterization of the model and its comparison to human pathology. Furthermore, males showed statistically higher IOP values ($p < 0.05$) than females, which can be explained by hormonal factors (estrogen receptors in females may improve vascular regulation and aqueous humor drainage, resulting in lower IOP levels), structural differences (males are predisposed to greater fibrosis of the trabecular meshwork, where dexamethasone acts), and the specific characteristics of the itself glaucoma model (the dexamethasone and dexamethasone combined with fibronectin models exhibited differences suggesting an interaction between the components in the inflammatory response) (Rodrigo *et al.* 2024). These differences highlight the importance of considering sex as a critical factor in glaucoma model research and in the development of personalized therapies.

The IV injection of KMLVE MSs reduced IOP in glaucomatous animals at 24 weeks following two 2 injections. After an initial hypertensive peak, one month after the first IV administration (6-week study), a decrease of IOP was observed, reaching significant IOP decrease at 10 weeks of the first IV injection (12 weeks of study). At 18 weeks of study (16 weeks of the first IV injection and 4 weeks of the second IV injection) the IOP was reduced until it reached normotensive values (healthy values), possibly because of a sum effect of latanoprost released in the two injections. Other authors have recently also explored the intravitreal administration of latanoprost as hypotensive drugs (Jukarainen *et al.* 2024). The delay in the hypotensive effect of latanoprost is not unexpected, considering that being a very hydrophobic compound, it must need time to diffuse throw the vitreous to its site of action. Furthermore, as a isopropyl ester prodrug it would need to undergo de-esterification to become the active metabolite. These results suggest that a higher latanoprost loading and further release is needed to obtain a significant hypotensive effect from the beginning of the treatment.

A functional improvement in latency of bipolar cells was detected at 12 weeks (10 weeks after IV) when ketorolac and melatonin might be close to being completely released according to *in vitro* studies. An increase in amplitude coinciding with IOP decreasing to normotension levels at 24 weeks was also observed. Furthermore, the decrease in IOP coincided with an improvement in retinal ganglion cells functionality at the end of the study, compared to non-treated glaucoma induced animals. In addition, this observation agreed with a normalization of gliosis, that may contribute to improved neuronal function. According to functional enhance, the neuroretinal structure measured by OCT did show a greater thickness than the rest of the cohorts, both in the retina as a whole and in the RGCs and their axons -the retinal nerve fiber layer- in the inner sectors closest to the optic nerve head. However, the treated glaucomatous eyes always presented worse records than their contralateral eyes and did not reach the thickness values observed for healthy animals.

From an ophthalmic point of view, the most striking finding of the study is the tangible normalization of gliosis. Ocular hypertension may induce Müller cells to become reactive and hypertrophic and able to produce mediators to enhance neuronal survival (Adornetto *et al.* 2019). Animals were induced with glaucoma, using a very slow and progressive model, which developed significant gliosis with a trend of RGC loss only 24 weeks after induction. This large gliosis may have been the reason for not finding a significant loss of RGCs despite reduced ERG responses, as it might be affecting neuronal activity. GFAP is an important marker of Müller cell activation. Müller cells express melatonin receptors, that's why melatoninergic agents may have an important impact on Müller cell activation. In this regard, multiple studies have demonstrated the anti-gliotic effect of melatonin under conditions of hypoxia, ischemia (Borlongan *et al.* 2000), surgery (Golabchi *et al.* 2018) or toxicity in the brain (Baydas, Reiter, Nedzvetskii, *et al.* 2003a), but also diabetes (Baydas, Reiter, Yasar, *et al.* 2003b, Baydas *et al.* 2004, Tu *et al.* 2020), hypercaloric diet (Dorranipour *et al.* 2024) or photoreceptor degeneration (Xu *et al.* 2017) and ocular hypertension (Dal Monte *et al.* 2020) coinciding with the robust results of our study. On the other hand, there is contradictory evidence regarding the rescue of RGC using melatonin. Models of retinopathy did detect rescue (Jiang *et al.* 2016), but in rat models of ocular hypertension by cauterization of episcleral veins also failed to protect (Marangoz *et al.* 2018), as in our results. Difference in the doses and in the pathological models could be responsible for contrasting results. Finally, there was no previous evidence in the scientific literature of normalization of gliosis with ketorolac and latanoprost, so this antigliotic finding of the IV formulation KMLVE could be probably attributed to melatonin.

Although further studies are necessary to clarify these hypotheses, all these results together suggest that the retinal recovery observed in the chronic glaucoma model was due to the early anti-inflammatory and neuroprotective effect of ketorolac and melatonin, and a later hypotensive effect of latanoprost. In this sense, although trying to postulate the neuroprotective activity of latanoprost in a model of glaucomatous retinal degeneration induced by ocular hypertension is complicated, it should not be forgotten that this compound can also have a neuroprotective effect, together with melatonin and ketorolac, each of them protecting the RGCs by different mechanisms, even if no hypotensive effect was measured at the beginning of the treatment.

Limitations and future studies: limitations inherent to working with animal models. Physiological differences between rats and humans, such as the absence of a macula in rodents, limit the direct extrapolation of the results. Additionally, while the model allows the observation of both intraocular pressure-dependent and independent effects, the interaction between neuroprotective and hypotensive mechanisms in humans may differ due to the involvement of multiple still-unknown pathways. Furthermore the quantification of pharmacokinetic levels in the eye, and comparison with independent cohorts treated with each of the drugs separately, could help to show the influence of each drug on neuroretina. Furthermore, an earlier release of latanoprost might be necessary to counteract the early hypertensive peak observed in this study.

5. Conclusions

It has been possible to successfully encapsulate in the same microsphere anti-inflammatory, antioxidant and hypotensive drugs (ketorolac, melatonin and latanoprost) and subsequently release them in a sustained manner. The IV formulation KMLVE enhanced neuroretinal functionality, rescued gliosis and decreased the intraocular pressure levels at the end of the study (6 months), comparing with non-treated glaucomatous animals This tri-delivery IODDS is a potential platform for the multifactorial treatment of glaucoma.

Acknowledgements

The authors would like to acknowledge the use of Servicio General a la Investigación-SAI, Universidad de Zaragoza. The authors are also grateful to Centro de Microscopía Electrónica Luis Bru (CAI, UCM), for technical SEM assistance. Miriam Ana González-Cela Casamayor and Marco Brugnera thank for their Ph.D. courses Spanish MECD (Reference FPU18/03445) and 813440-ORBITAL-H2020-MSCA-ITN-2018 fellowships, respectively.

Author contributions

CRediT: **Miriam González-Cela Casamayor**: Data curation, Formal analysis, Investigation, Methodology, Software, Validation, Writing – original draft; **María J. Rodrigo**: Conceptualization, Formal analysis, Funding acquisition, Investigation, Methodology, Project administration, Resources, Software, Supervision, Validation, Visualization, Writing – original draft, Writing – review & editing; **Marco Brugnera**: Formal analysis, Investigation, Methodology, Visualization, Writing – review & editing; **Inés Munuera**: Data curation, Formal analysis, Investigation, Methodology, Writing – original draft; **Teresa Martínez-Rincón**: Formal analysis, Investigation, Methodology, Writing – original draft; **Catalina Prats-Lluís**: Investigation; **Pilar Villacampa**: Conceptualization, Investigation, Validation, Visualization, Writing – review & editing; **Julián García Feijoo**: Investigation, Conceptualization; **Luis E. Pablo**: Conceptualization, Formal analysis, Investigation, Project administration, Resources; **Irene Bravo-Osuna**: Conceptualization, Funding acquisition, Investigation, Project administration, Resources, Supervision, Validation, Visualization, Writing – review & editing; **Elena Garcia-Martin**: Conceptualization, Formal analysis, Investigation, Software, Supervision, Validation, Visualization, Writing – review & editing; **Rocío Herrero-Vanrell**: Conceptualization, Funding acquisition, Investigation, Project administration, Resources, Supervision, Validation, Visualization, Writing – review & editing.

Ethical approval

The use of animals is justified by the need to reproduce pathological conditions in a living system. *Ex vivo* studies would be insufficient to evaluate the efficacy of the treatment. A total of 82 Long-Evans rats (41 males and 41 females), aged 4 weeks and weighing between 50-100 g at the start of the study, were employed. The animals were housed in standard cages, with food and water provided *ad libitum*. Environmental conditions were carefully controlled, including a 12-hour light/dark cycle, a temperature of 22 °C, and a relative humidity of 55%. For corneal, IV injections and IOP measurements, rats were sedated with 3% sevoflurane gas in 1.5% oxygen. The animals were then recovered in a chamber enriched with 2% oxygen and controlled temperature. For ERG and OCT acquisitions, general anesthesia was induced via intraperitoneal injections of ketamine (60 mg/kg) and dexmedetomidine (0.25 mg/kg). The animals were humanely euthanized with an intracardiac injection of sodium tiopenthal (25 mg/mL) under general anesthesia. All procedures involving animals were conducted in compliance with the Association for Research in Vision and Ophthalmology (ARVO) guidelines on animal use and were approved by the Ethics Committee for Animal Research (P179/20). Furthermore, the authors adhered to the ARRIVE (Animal Research: Reporting of *In Vivo* Experiments) guidelines.

Author contributions

Conceptualization: Rocío Herrero-Vanrell, Irene Bravo-Osuna, MJ. Rodrigo, Elena Garcia-Martin, Luis E Pablo, Julián García Feijoo, Pilar Villacampa; Data curation: Miriam Ana González-Cela Casamayor; Inés Munuera; Formal analysis: Miriam Ana Gonzalez-Cela-Casamayor, Marco Brugnera, Inés Munuera, Teresa Martínez-Rincón, Elena Garcia-Martin, MJ. Rodrigo; Funding acquisition: Rocío Herrero-Vanrell, Irene Bravo-Osuna, MJ. Rodrigo, Luis E Pablo; Investigation: Miriam Ana Gonzalez-Cela-Casamayor, Marco Brugnera, Rocío Herrero-Vanrell, Irene Bravo-Osuna, MJ. Rodrigo, Inés Munuera, Elena Garcia-Martin, Luis E Pablo, Julián García Feijoo, Teresa Martínez-Rincón, Catalina Prats-Lluís, Pilar Villacampa; Methodology: Miriam Ana Gonzalez-Cela Casamayor, Marco Brugnera, MJ. Rodrigo, Inés Munuera, Teresa Martínez-Rincón; Project administration: Rocío Herrero-Vanrell, Irene Bravo-Osuna, MJ. Rodrigo, Luis E Pablo; Resources: Rocío Herrero-Vanrell, Irene Bravo-Osuna, MJ. Rodrigo, Luis E Pablo; Software: Miriam Ana González-Cela Casamayor, MJ. Rodrigo, Elena Garcia-Martin; Supervision: Rocío Herrero-Vanrell, Irene Bravo-Osuna, MJ. Rodrigo, Elena Garcia-Martin; Validation: Miriam Ana González-Cela Casamayor, Rocío Herrero-Vanrell, Irene Bravo-Osuna, MJ. Rodrigo, Elena Garcia-Martin, Pilar Villacampa; Visualization: Marco Brugnera, Irene Bravo-Osuna, Rocío Herrero-Vanrell, MJ. Rodrigo, Elena Garcia-Martin, Pilar Villacampa; Writing – original draft: Miriam Ana González-Cela Casamayor, MJ. Rodrigo, Inés Munuera, Teresa Martínez-Rincón; Writing – review & editing: Marco Brugnera, Irene Bravo-Osuna, Rocío Herrero-Vanrell, MJ. Rodrigo, Elena Garcia-Martin, Pilar Villacampa.

Disclosure statement

No potential conflict of interest was reported by the author(s).

Funding

This work was supported by Juan Rodés Research Grant JR22/00057, RD21/0002/0050, RD24/0007/0022 (Instituto de Salud Carlos III) Grants, PID2020-113281RB-C21, PID2020-113281RB-C22, PID2023-148219OB-C21 and PID2023-148219OB-C22 funded by MCIN/AEI/10.13039/501100011033 and 813440-ORBITAL-H2020-MSCA-ITN-2018 (This project was funded by the European Union's Horizon 2020 Research and Innovation Programme under the Marie Sklodowska–Curie Actions grant agreement number 813440 (Ocular Research by Integrated Training and Learning (ORBITAL)).

ORCID

Miriam Ana González-Cela-Casamayor http://orcid.org/0000-0001-6694-9700
María J. Rodrigo http://orcid.org/0000-0002-4009-3075
Marco Brugnera http://orcid.org/0000-0003-2600-6446
Inés Munuera http://orcid.org/0000-0002-1502-641X
Teresa Martínez-Rincón http://orcid.org/0000-0002-8891-0417
Pilar Villacampa http://orcid.org/0000-0002-2860-7475
Julián García-Feijoo http://orcid.org/0000-0002-7772-5718
Luis E. Pablo http://orcid.org/0000-0003-2389-8282
Irene Bravo-Osuna http://orcid.org/0000-0003-3133-7872
Elena Garcia-Martin http://orcid.org/0000-0001-6258-2489
Rocío Herrero-Vanrell http://orcid.org/0000-0001-9764-7975

Data availability statement

Data will be available upon request to the corresponding author.

References

Actis, A.G., and Rolle, T., 2014. Ocular surface alterations and topical antiglaucomatous therapy: A review. *The open ophthalmology journal*, 8, 67–72. doi: 10.2174/1874364101408010067.

Adornetto, A., Russo, R., and Parisi, V., 2019. Neuroinflammation as a target for glaucoma therapy. *Neural regeneration research*, 14 (3), 391–394. doi: 10.4103/1673-5374.245465.

Alhalafi, A. M., 2017. Applications of polymers in intraocular drug delivery systems. Oman ophthalmic society, *10*, 3–8. doi: 10.4103/0974-620X.200692.

Alm, A., 2014. Latanoprost in the treatment of glaucoma. *Clinical ophthalmology (Auckland, N.Z.)*, 8, 1967–1985. doi: 10.2147/OPTH.S59162.

Aragón-Navas, A., *et al.*, 2022. Mimicking chronic glaucoma over 6 months with a single intracameral injection of dexamethasone/fibronectin-loaded PLGA microspheres. *Drug delivery*, 29 (1), 2357–2374. doi: 10.1080/10717544.2022.2096712.

Arranz-romera, A., *et al.*, 2019. Simultaneous co-delivery of neuroprotective drugs from multi-loaded PLGA microspheres for the treatment of glaucoma. *Journal of controlled release: official journal of the controlled release society*, 297 (January), 26–38. doi: 10.1016/j.jconrel.2019.01.012.

Arranz-Romera, A., *et al.*, 2021. Co-delivery of glial cell–derived neurotrophic factor (GDNF) and tauroursodeoxycholic acid (TUDCA) from PLGA microspheres: potential combination therapy for retinal diseases. *Drug delivery and translational research*, 11 (2), 566–580. doi: 10.1007/s13346-021-00930-9.

Arrighi, A., *et al.*, 2019. Development of PLGA microparticles with high immunoglobulin G-loaded levels and sustained-release properties obtained by spray-drying a water-in-oil emulsion. *International journal of pharmaceutics*, 566 (February), 291–298. doi: 10.1016/j.ijpharm.2019.05.070.

Barbosa-Alfaro, D., *et al.*, 2021. Dexamethasone plga microspheres for sub-tenon administration: Influence of sterilization and tolerance studies. *Pharmaceutics*, 13 (2), 228. doi: 10.3390/pharmaceutics13020228.

Baydas, G., *et al.*, 2003a. Melatonin protects the central nervous system of rats against toluene-containing thinner intoxication by reducing reactive gliosis. *Toxicology letters*, 137 (3), 169–174. doi: 10.1016/S0378-4274(02)00400-9.

Baydas, G., *et al.*, 2003b. Melatonin reduces glial reactivity in the hippocampus, cortex, and cerebellum of streptozotocin-induced diabetic rats. *Free radical biology & medicine*, 35 (7), 797–804. doi: 10.1016/S0891-5849(03)00408-8.

Baydas, G., *et al.*, 2004. Early changes in glial reactivity and lipid peroxidation in diabetic rat retina: effects of melatonin. *Acta diabetologica*, 41 (3), 123–128. doi: 10.1007/s00592-004-0155-x.

Belforte, N.A., *et al.*, 2010. Melatonin: a novel neuroprotectant for the treatment of glaucoma. *Journal of pineal research*, 48 (4), 353–364. doi: 10.1111/j.1600-079X.2010.00762.x.

Bessone, C.D.V., *et al.*, 2020. Neuroprotective effect of melatonin loaded in ethylcellulose nanoparticles applied topically in a retinal degeneration model in rabbits. *Experimental eye research*, 200 (April), 108222. doi: 10.1016/j.exer.2020.108222.

Bessone, V., *et al.*, 2019. Protective role of melatonin on retinal ganglionar cell: in vitro an in vivo evidences. *Life sci [internet]*, 218, 233–240. doi: 10.1016/j.lfs.2018.12.053.

Bhanu, M., Harsha, K., and Anupam, P., 2017. Ocular drug delivery systems. *Natural polymer drug delivery*, 160–170. doi: 10.1079/9781780644479.0160.

Borlongan, C.V., *et al.*, 2000. Glial cell survival is enhanced during melatonin-induced neuroprotection against cerebral ischemia. *FASEB journal: official publication of the federation of American societies for experimental biology*, 14 (10), 1307–1317. doi: 10.1096/fj.14.10.1307.

Bravo-osuna, I., *et al.*, 2018. Microspheres as intraocular therapeutic tools in chronic diseases of the optic nerve and retina. *Advanced drug delivery reviews*, 126, 127–144. doi: 10.1016/j.addr.2018.01.007.

Brugnera, M., *et al.*, 2022. Validation of a rapid and easy-to-apply method to simultaneously quantify co-loaded dexamethasone and melatonin PLGA microspheres by HPLC-UV: encapsulation efficiency and in vitro release. *Pharmaceutics*, 14 (2), 288. doi: 10.3390/pharmaceutics14020288.

Checa-Casalengua, P., *et al.*, 2011. Retinal ganglion cells survival in a glaucoma model by GDNF/Vit e PLGA microspheres prepared according to a novel microencapsulation procedure. *Journal of controlled release: official journal of the controlled release society*, 156 (1), 92–100. doi: 10.1016/j.jconrel.2011.06.023.

Chidlow, G., Wood, J.P.M., and Casson, R.J., 2007. Pharmacological neuroprotection for glaucoma. *Drugs*, 67 (5), 725–759. doi: 10.2165/00003495-200767050-00006.

Costagliola, C., *et al.*, 2008. Topical and oral ketorolac administration increases the intraocular pressure-lowering effect of latanoprost. *Current eye research*, 33 (5), 477–482. doi: 10.1080/02713680802100845.

Dal Monte, M., *et al.*, 2020. A topical formulation of melatoninergic compounds exerts strong hypotensive and neuroprotective effects in a rat model of hypertensive glaucoma. *International journal of molecular sciences*, 21 (23), 9267. doi: 10.3390/ijms21239267.

Davies, N.M., 2000. Biopharmaceutical considerations in topical ocular drug delivery. *Clinical and experimental pharmacology & physiology*, 27 (7), 558–562. doi: 10.1046/j.1440-1681.2000.03288.x.

del Amo, E.M., 2022. Topical ophthalmic administration: Can a drug instilled onto the ocular surface exert an effect at the back of the eye? *Frontiers in drug delivery*, 2, 1–16. doi: 10.3389/fddev.2022.954771.

Dorranipour, D., *et al.*, 2024. Astrocyte response to melatonin treatment in rats under high-carbohydrate high-fat diet. *Journal of chemical neuroanatomy*, 136, 102389. doi: 10.1016/j.jchemneu.2024.102389.

Doucette, L.P., and Walter, M.A., 2017. Prostaglandins in the eye: Function, expression, and roles in glaucoma Prostaglandins in the eye: Function, expression, and roles in glaucoma. *Ophthalmic genetics*, 38 (2), 108–116. doi: 10.3109/13816810.2016.1164193.

Drago, F., *et al.*, 2001. Latanoprost Exerts Neuroprotective Activity in vitro and in vivo. *Experimental eye research*, 72 (4), 479–486. doi: 10.1006/exer.2000.0975.

García-Caballero, C., *et al.*, 2017. European Journal of Pharmaceutical Sciences Six month delivery of GDNF from PLGA/vitamin E biodegradable microspheres after intravitreal injection in rabbits. *European journal of pharmaceutical sciences: official journal of the european federation for pharmaceutical sciences*, 103, 19–26. doi: 10.1016/j.ejps.2017.02.037.

García-Caballero, C., *et al.*, 2018. Photoreceptor preservation induced by intravitreal controlled delivery of GDNF and GDNF/melatonin in rhodopsin knockout mice. *Molecular vision*, 24 (November), 733–745.

Ghosh, S., *et al.*, 2024. Design of highly adhesive urchin-like gold nanostructures for effective topical drug administration and symptomatic relief of corneal dryness. *Small struct*, 2400484. doi: 10.1002/sstr.202400484.

Golabchi, A., *et al.*, 2018. Melatonin improves quality and longevity of chronic neural recording. *Biomaterials [internet]*, 180, 225–239. doi: 10.1016/j.biomaterials.2018.07.026.

Herrero-Vanrell, R., *et al.*, 2014. The potential of using biodegradable microspheres in retinal diseases and other intraocular pathologies. *Progress in retinal and eye research*, 42, 27–43. doi: 10.1016/j.preteyeres.2014.04.002.

Horne, R.R., Judd, K.E., and Pitt, W.G., 2017. Rapid loading and prolonged release of latanoprost from a silicone hydrogel contact lens. *Journal of drug delivery science and technology [internet]*, 41, 410–418. doi: 10.1016/j.jddst.2017.08.011.

López-Cano, J.L., *et al.*, 2021. Thermo-responsive PLGA-PEG-PLGA hydrogels as novel injectable platforms for neuroprotective combined therapies in the treatment of retinal degenerative diseases. *Pharmaceutics*, 13(2), 234.

Jiang, C., *et al.*, 2007. Intravitreal injections of GDNF-loaded biodegradable microspheres are neuroprotective in a rat model of glaucoma. *Molecular vision*, 13, 1783–1792.

Jiang, T., *et al.*, 2016. Protective effects of melatonin on retinal inflammation and oxidative stress in experimental diabetic retinopathy. *Oxidative medicine and cellular longevity*, 2016, 14–17. doi: 10.1155/2016/3528274.

Jukarainen, H. J., *et al.*, 2024. Safety, tolerability & pharmacokinetics of sustained release Latanoprost (LAT) from intravitreal injection of a semi-solid in-situ forming implant. *Investigative Ophthalmology & Visual Science,* 65, 3981.

Kanamori, A., *et al.*, 2009. Latanoprost protects rat retinal ganglion cells from apoptosis in vitro and in vivo. *Experimental eye research*, 88 (3), 535–541. doi: 10.1016/j.exer.2008.11.012.

Kudo, H., *et al.*, 2006. Neuroprotective effect of latanoprost on rat retinal ganglion cells: 1003–1009. doi: 10.1007/s00417-005-0215-0.

Lee, A.J., and Goldberg, I., 2011. Emerging drugs for ocular hypertension. *Expert opinion on emerging drugs*, 16 (1), 137–161. doi: 10.1517/14728214.2011.521631.

Makadia, H.K., and Siegel, S.J., 2011. Poly lactic-co-glycolic acid (PLGA) as biodegradable controlled drug delivery carrier. *Polymers*, 3 (3), 1377–1397. doi: 10.3390/polym3031377.

Mansoor, S., and Tas, C., 2014. Simple, fast, and sensitive isocratic high-performance liquid chromatography method for the quantification of latanoprost. *Acta chromatographica*, 26 (2), 191–202. doi: 10.1556/AChrom.26.2014.2.1.

Marangoz, D., *et al.*, 2018. Comparison of the neuroprotective effects of brimonidine tartrate and melatonin on retinal ganglion cells. *International ophthalmology*, 38 (6), 2553–2562. doi: 10.1007/s10792-017-0768-z.

Maranha, R.C., 2020. Nanotechnology for medical and surgical glaucoma therapy—a review. *Advances in therapy*, 37, 155–199. doi: 10.1007/s12325-019-01163-6.

Meier-gibbons, F., and Marc, T., 2020. Influence of cost of care and adherence in glaucoma management: an update. *Journal of Ophthalmology*.

Mietzner, R., *et al.*, 2020. Fasudil loaded PLGA microspheres as potential intravitreal depot formulation for glaucoma therapy. *Pharmaceutics*, 12 (8), 706. doi: 10.3390/pharmaceutics12080706.

Nadal-Nicolás, F.M., *et al.*, 2016. Ketorolac administration attenuates retinal ganglion cell death after axonal injury. *Investigative ophthalmology & visual science*, 57 (3), 1183–1192. doi: 10.1167/iovs.15-18213.

Nguyen, D.D., Luo, L.J., and Lai, J.Y., 2020. Effects of shell thickness of hollow poly(lactic acid) nanoparticles on sustained drug delivery for pharmacological treatment of glaucoma. *Acta biomaterialia*, 111, 302–315. doi: 10.1016/j.actbio.2020.04.055.

Nieto, K., Mallery, S.R., and Schwendeman, S.P., 2020. Microencapsulation of amorphous solid dispersions of fenretinide enhances drug solubility and release from PLGA in vitro and in vivo. *International journal of pharmaceutics*, 586 (May), 119475. doi: 10.1016/j.ijpharm.2020.119475.

Pan, X., *et al.*, 2020. Co-delivery of dexamethasone and melatonin by drugs laden PLGA nanoparticles for the treatment of glaucoma. *Journal of drug delivery science and technology [internet]*, 60 (August), 102086. doi: 10.1016/j.jddst.2020.102086.

Park, C.W., *et al.*, 2018. Preparation and in vitro/in vivo evaluation of PLGA microspheres containing norquetiapine for long-acting injection. *Drug design, development and therapy*, 12, 711–719. doi: 10.2147/DDDT.S151437.

Reiter, R.J., *et al.*, 2016. Melatonin as an antioxidant: under promises but over delivers. *Journal of pineal research*, 61 (3), 253–278. doi: 10.1111/jpi.12360.

Review, C., 2014. The pathophysiology and treatment of glaucoma. a review. *Clinical review education*, 311 (18), 1901–1911. doi: 10.1001/jama.2014.3192.

Rodrigo, M.J., *et al.*, 2024. Influence of sex on chronic steroid-induced glaucoma: 24-Weeks follow-up study in rats. *Experimental eye research*, 238, 109736. doi: 10.1016/j.exer.2023.109736.

Saniples, J.R., Krause, G., and Lewy, A.J., 2000. Effect of melatonin on intraocular pressure. *Current eye research*, 7 (7), 649–653.

Shirley, M., 2020. Bimatoprost implant: first approval. *Drugs & aging*, 37 (7), 549. doi: 10.1007/s40266-020-00769-8.

Sirinek, P.E., *et al.*, 2022. Seminars in Ophthalmology Intracameral sustained release bimatoprost implants (Durysta) Intracameral sustained release bimatoprost implants (Durysta) ABSTRACT. *Seminars in ophthalmology*, 37 (3), 385–390. doi: 10.1080/08820538.2021.1985145.

Tanito, M., *et al.*, 2018. Different glaucoma types and glaucoma surgeries among different age groups. *Graefe's archive for clinical and experimental ophthalmology = albrecht von graefes archiv fur klinische und experimentelle ophthalmologie*, 256 (10), 2013–2014. doi: 10.1007/s00417-018-4058-x.

Traber, M.G., and Atkinson, J., 2007. Vitamin E, antioxidant and nothing more. *Free radical biology & medicine*, 43 (1), 4–15. doi: 10.1016/j.freeradbiomed.2007.03.024.

Tu, Y., *et al.*, 2020. Melatonin inhibits Müller cell activation and pro-inflammatory cytokine production via upregulating the MEG3/miR-204/Sirt1 axis in experimental diabetic retinopathy. *Journal of cellular physiology*, 235 (11), 8724–8735. doi: 10.1002/jcp.29716.

Turan-Vural, E., Torun-Acar, B., and Acar, S., 2012. Effect of ketorolac add-on treatment on intra-ocular pressure in glaucoma patients receiving prostaglandin analogues. *Ophthalmologica. Journal international d'ophtalmologie. International journal of ophthalmology. Zeitschrift fur augenheilkunde*, 227 (4), 205–209. doi: 10.1159/000333822.

Wang, Y., *et al.*, 2021. FDA's poly (lactic-co-glycolic acid) research program and regulatory outcomes. *The AAPS journal*, 23 (4), 92. doi: 10.1208/s12248-021-00611-y.

Xu, X.J., *et al.*, 2017. Melatonin delays photoreceptor degeneration in a mouse model of autosomal recessive retinitis pigmentosa. *Journal of pineal research*, 63 (3), 1–12. doi: 10.1111/jpi.12428.

Yamamoto, K., *et al.*, 2017. The neuroprotective effect of latanoprost acts via klotho-mediated suppression of calpain activation after optic nerve transection. *Journal of neurochemistry*, 140 (3), 495–508. doi: 10.1111/jnc.13902.

Ye, D., *et al.*, 2022. Anti - PANoptosis is involved in neuroprotective effects of melatonin in acute ocular hypertension model. *Journal of pineal research*, 73(4), e12828. doi: 10.1111/jpi.12828.

Zhao, M., *et al.*, 2017. Tolerance of high and low amounts of PLGA microspheres loaded with mineralocorticoid receptor antagonist in retinal target site. *Journal of controlled release: official journal of the controlled release society*, 266, 187–197. doi: 10.1016/j.jconrel.2017.09.029.